



**HAL**  
open science

# Powerful Protein Nanoreservoirs Based on Stellate Mesoporous Silica Embedded in Composite Hydrogels: From Burst Release to Retention

Joelle Bizeau, Morgane Rabineau, Julie Buisson, Theo Lucante, Cedric Leuvrey, Ksenia Parkhomenko, Philippe Lavalley, Damien Mertz

► **To cite this version:**

Joelle Bizeau, Morgane Rabineau, Julie Buisson, Theo Lucante, Cedric Leuvrey, et al.. Powerful Protein Nanoreservoirs Based on Stellate Mesoporous Silica Embedded in Composite Hydrogels: From Burst Release to Retention. *Macromolecular Chemistry and Physics*, In press, 10.1002/macp.202400035 . hal-04570229

**HAL Id: hal-04570229**

**<https://hal.science/hal-04570229>**

Submitted on 6 May 2024

**HAL** is a multi-disciplinary open access archive for the deposit and dissemination of scientific research documents, whether they are published or not. The documents may come from teaching and research institutions in France or abroad, or from public or private research centers.

L'archive ouverte pluridisciplinaire **HAL**, est destinée au dépôt et à la diffusion de documents scientifiques de niveau recherche, publiés ou non, émanant des établissements d'enseignement et de recherche français ou étrangers, des laboratoires publics ou privés.

# Powerful Protein Nanoreservoirs Based on Stellate Mesoporous Silica Embedded in Composite Hydrogels: From Burst Release to Retention

Joëlle Bizeau, Morgane Rabineau, Julie Buisson, Théo Lucante, Cédric Leuvrey, Ksenia Parkhomenko, Philippe Lavalle, and Damien Mertz\*

In the biomaterials field, one major issue with hydrogels (HGs) loaded with active therapeutics is the spontaneous leaking of the cargo occurring rapidly, usually over several hours. However, biological processes involved in regenerative medicine would require to have a sustained drug delivery lasting over weeks/months or be triggered only when a specific biochemical stimulus (enzymatic, cellular, or antimicrobial) is applied. In this work, this challenge is addressed by demonstrating that the spontaneous protein release from an agarose HG (used as model HG) can be partially or totally blocked by the incorporation of stellate mesoporous silica (STMS) nanoparticles (NPs,  $\approx 150 \pm 28$  nm size, 15 nm pore) within the HG. It is shown here that the porous silica NPs act as sub-micrometer size reservoirs ensuring precise level retention simply by playing on the amount of STMS embedded in the HG. Further, this effect is shown for various proteins demonstrating the versatility of this concept.

Indeed, the endogenous source of these bio-macromolecules makes them intrinsically biocompatible and biodegradable with non-toxic degradation products, and their involvement in a lot of biological processes allows their use in a wide range of therapeutic applications (cancer therapy, diabetes treatment, tissue engineering, etc.). The disadvantages of using such bio-macromolecules are also well known (short half-life, poor membrane permeability, and conformational fragility) and led to the development of a lot of protein delivery systems (PDSs) to counteract these drawbacks.<sup>[1–4]</sup>

Among the possible PDS formulations, hydrogels (HGs) present a certain interest in the delivery of proteins for tissue engineering as they are 3D polymer networks able to absorb a high amount of water.

This ability makes them quite suitable for

the encapsulation of proteins as their water pockets provide a hydrophilic environment that can encapsulate them while protecting them, which notably avoids their denaturation and loss of biological activity.<sup>[5–7]</sup> In addition, HGs are quite easily tunable, as their water absorption capacity and viscoelasticity can be modulated by playing on the cross-linking density of the polymer, which is already a challenge to perform without using toxic molecules.<sup>[8,9]</sup> However, a huge challenge that researchers are still facing when developing HG for protein delivery, and drug delivery in general, is to avoid the spontaneous leakage of the therapeutic molecule due to the loading strategy.<sup>[6]</sup> Indeed, the molecules are loaded in the water pockets, but these are usually of a higher size and do not retain the therapeutic molecules. Specific efforts should thus be put in the development of HGs able to finely control the release of proteins in order to avoid a burst release that would empty the system too quickly and may lead to negative side effects due to the presence of a too high amount of proteins.<sup>[10]</sup>

To our knowledge, most of the HGs are developed to get a sustained release, which is still an improvement compared to the injection of aqueous solutions of protein.<sup>[11]</sup> The strategies reported are mainly to render the HGs sensitive to internal (temperature, pH, ionic strength, etc.)<sup>[5–7,11,12]</sup> or external stimuli.<sup>[13,14]</sup> Some articles also use the protein immobilization into the HGs, as reported by Wang et al. who developed a photoresponsive HGs by using the ability of the C-terminal adenosylcobalamin binding


## 1. Introduction

Proteins have been studied as therapeutic agents since decades as they present several advantages compared to synthesized drugs.

J. Bizeau, T. Lucante, C. Leuvrey, D. Mertz  
 Institut de Physique et Chimie des Matériaux de Strasbourg (IPCMS)  
 UMR-7504 CNRS-Université de Strasbourg  
 23 rue du Loëss, BP 34, Strasbourg Cedex 2 67034, France  
 E-mail: [damien.mertz@ipcms.unistra.fr](mailto:damien.mertz@ipcms.unistra.fr)

M. Rabineau, J. Buisson, P. Lavalle  
 Inserm UMR\_S 1121, CNRS EMR 7003, Université de Strasbourg, Biomaterials and Bioengineering  
 Inserm UMR\_S 1121 Biomaterials and Bioengineering  
 Centre de Recherche en Biomédecine de Strasbourg  
 1 Rue Eugène Boeckel, Strasbourg 67084, France

K. Parkhomenko  
 Institut de Chimie des Procédés pour l'Energie  
 l'Environnement et la Santé (ICPEES)  
 UMR-7515 CNRS-Université de Strasbourg  
 25 rue Becquerel, Strasbourg 67087, France

 The ORCID identification number(s) for the author(s) of this article can be found under <https://doi.org/10.1002/macp.202400035>

© 2024 The Authors. Macromolecular Chemistry and Physics published by Wiley-VCH GmbH. This is an open access article under the terms of the [Creative Commons Attribution-NonCommercial](https://creativecommons.org/licenses/by-nc/4.0/) License, which permits use, distribution and reproduction in any medium, provided the original work is properly cited and is not used for commercial purposes.

DOI: 10.1002/macp.202400035

domain in CarH protein to form a tetramer in the dark by binding to adenosylcobalamin AdoB12.<sup>[13]</sup> Other examples are the work reported by Zhang et al. in which they used the ability of aptamer to specifically bind to proteins<sup>[15]</sup> and the work reported by Delplace et al. who used the SH3 binding peptide.<sup>[16]</sup> An interesting work is the one reported by Awada et al. in which a fibrin HG was loaded with tissue inhibitor of metalloproteinases-3 (TIMP-3) and heparin-protein coacervates made with basic fibroblast growth factor (FGF-2) or stromal cell-derived factor-1 $\alpha$  (SDF-1 $\alpha$ ). This allowed the desired burst release of TIMP-3 while FGF-2 and SDF-1 $\alpha$  were slowly and continuously released for a better cardiac tissue regeneration.<sup>[17]</sup> Another strategy is to develop composite HGs by including a nanomaterial in this structure, which has been reported with poly(lactic-co-glycolic acid) (PLGA) nanoparticles (NPs),<sup>[18]</sup> heparin microparticles,<sup>[19]</sup> poly(lactic acid) (PLA) short electrospun fibers,<sup>[20]</sup> and nanosilicates.<sup>[21]</sup> However, most of the release profiles reported in these studies present a burst release<sup>[6–11,16,18,22–26]</sup> and few actually works on reducing or even stopping it. Among the 26 papers checked, we found only four that worked in this direction, and they correspond to the one reporting composite systems,<sup>[18–20]</sup> except for the nanosilicates that were first used to improve the HGs' mechanical properties,<sup>[21]</sup> and the coacervate system.<sup>[17]</sup> For example, Dai et al. clearly express that they combine PLGA NPs and chitosan/ $\beta$ -glycerophosphate thermosensitive HGs for the delivery of protein to the inner ear to counteract the fast elimination of NPs and the protein fast leaking from HGs.<sup>[18]</sup>

There is thus a real need to develop new HG systems which would ensure controlled protein retention and ultimately desired controlled pulsatile release. To address this challenge, composite HGs in which a nanomaterial would be used as a protein reservoir embedded in an HG seem to be a promising route as they would better control the protein delivery but also increase the HG mechanical strength and can present external field-responsive properties if used activable nanoparticles.<sup>[27]</sup> Among the possible protein reservoirs, mesoporous silica micro- and nanoparticles are of particular interest as it is simple to synthesize via surfactant-assisted sol-gel methods, biocompatible and robust systems that were already reported for protein delivery.<sup>[1]</sup> More specifically, we reported the use of stellate mesoporous silica (STMS) nanoparticles, particularly suitable for macromolecule delivery as the pore size is around 15 nm,<sup>[28]</sup> for the sustained release of human serum albumin (HSA) and horseradish peroxidase (HRP) under dynamic conditions after the functionalization with isobutyramide, a moiety acting as a molecular glue.<sup>[29]</sup> Even if we reported the HG self-assembly of peptides fibers from enzyme bound to STMS quite recently,<sup>[30]</sup> no work to date envisioned the use of STMS as sub-micrometer size protein reservoirs.

Herein, with the aim to address the challenge of the spontaneous protein release from HGs, we investigated the ability of new composite HGs, made from STMS NPs dispersed in an agarose HG, to block and even to tune the spontaneous protein release (concept represented in **Scheme 1**). Agarose coming from agar-agar or agar-bearing marine algae was used here to produce model HGs as it is biocompatible, biodegradable, and cost-effective. In addition, agarose HGs are easily formed without covalent cross-linkers with easily tunable mechanical properties (elastic moduli), as they are linked to the agarose content.

We report here that incorporating STMS NPs allows us to switch the protein behavior from a spontaneous release without any particles to a total protein retention within the agarose HG using a high amount of NPs (5 wt%). In the first part, we investigated the effect of the NPs formulation within the HG to control the protein burst release or its retention using HSA as a model protein. In the second part, with the aim to demonstrate the versatility of the approach toward various proteins, three other proteins (enzymes) were studied in depth: HRP, alkaline phosphatase (ALP), and lysozyme (LYS). To validate the mechanism of protein retention where the STMS plays the role of sub-micrometer size protein reservoirs, HG structures bearing large pore silica microparticles and loaded with the four fluorescently labeled proteins were imaged in details by confocal microscopy. Then, the biological features of the proteins were investigated first using circular dichroism on the four proteins and second performing enzymatic activity tests on HRP and ALP. Even if the conformation of the four proteins seems to change while released from agarose HG, the enzymatic activity of HRP and ALP was found to be maintained whether these enzymes were released from an STMS-free agarose HG or immobilized on STMS NPs, showing the potential of such systems to be used for medical applications.

## 2. Results and Discussion

### 2.1. Effect of the STMS Amount within the HG on the Spontaneous Release of HSA

The first objective of this work was to evaluate the impact of the STMS content on the loading and spontaneous release of a model protein from an agarose/STMS composite HG. To do so, we decided to work with a fixed volume of HG of 2 mL at 1 wt% and a fixed amount of HSA of 2 mg. To evaluate the amount of loaded protein, we used the indirect method by quantifying the amount of unloaded protein in the loading supernatant (LS) and in the washing supernatant (WS) and converted it into the loading content (LC) defined as given in Equation (1)

$$LC (\mu\text{g mL}^{-1}) = \frac{m_{\text{loaded protein}}}{V_{\text{HG}}} = \frac{m_{\text{added protein}} - m_{\text{unloaded protein}}}{V_{\text{HG}}} \quad (1)$$

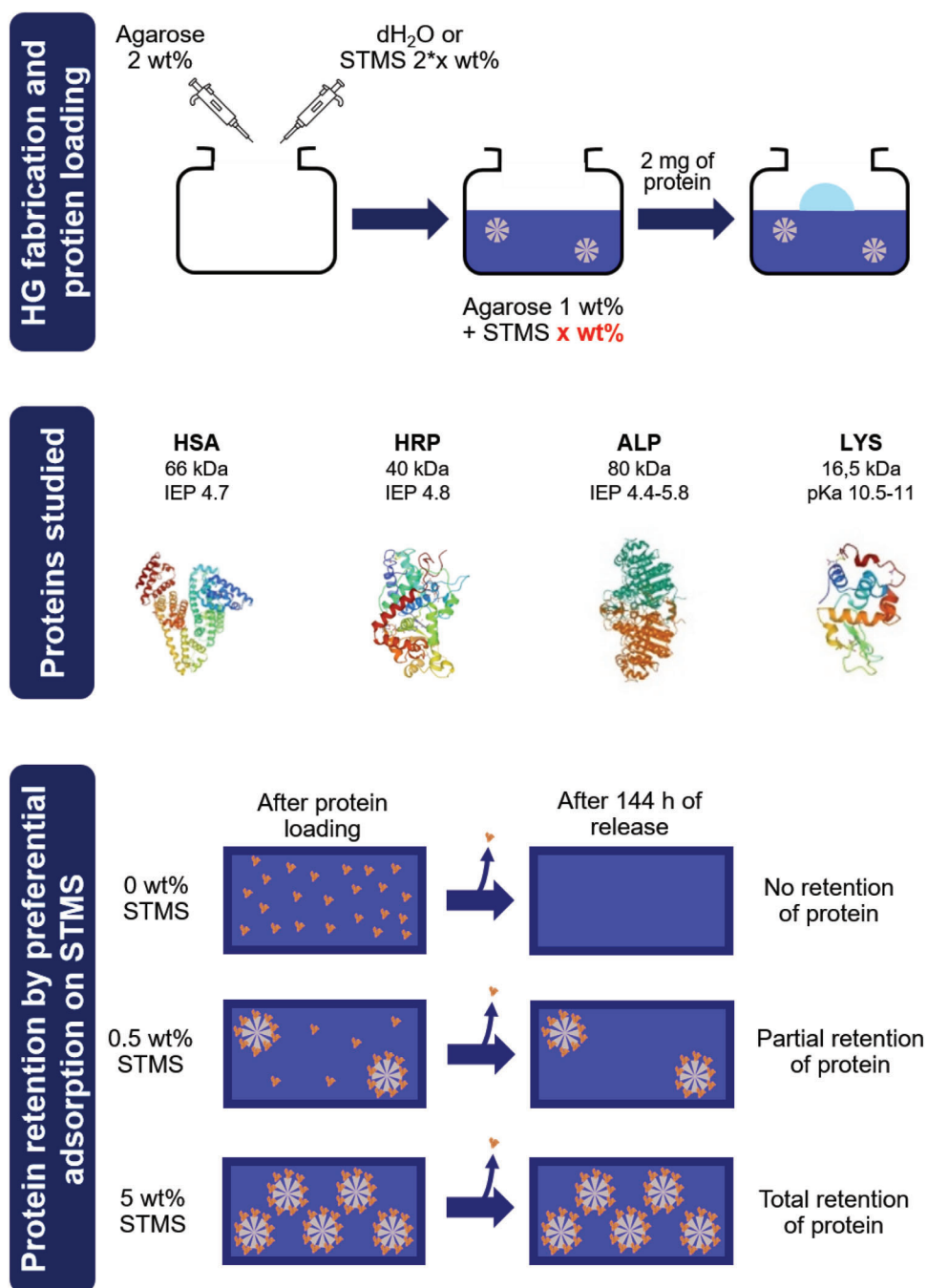
with  $m_{\text{loaded protein}}$  in  $\mu\text{g}$  and  $V_{\text{HG}}$  being the volume of HG in mL. We also defined the loading efficiency (LE) as given in Equation (2)

$$LE (\%) = \frac{m_{\text{loaded protein}}}{m_{\text{added protein}}} \times 100 \quad (2)$$

with all the masses in  $\mu\text{g}$ .

In addition, we choose the bicinchoninic acid (BCA) assay as quantification technique as it was shown to be one of the most powerful and robust techniques as compared to other methods.<sup>[29]</sup> The corresponding calibration curve in deionized water (dH<sub>2</sub>O) is given in Figure S1 (Supporting Information).

The STMS NPs with a size of  $\approx 150 \pm 28$  nm were synthesized and characterized as reported previously<sup>[29,35–37]</sup> (**Figure 1A–C**) and washed three times with dH<sub>2</sub>O prior to be used to fabricate the HGs. The composite HGs were then prepared by mixing



**Scheme 1.** Representative scheme of the study and its main results. Representation of HSA, HRP, ALP, and LYS provided by Protein Data Base by Sugio et al.,<sup>[31]</sup> Berglund et al.,<sup>[32]</sup> Kim and Wyckoff,<sup>[33]</sup> and Muraki et al.,<sup>[34]</sup> respectively.

equal volumes of a 2 wt% agarose solution and a 2\*x wt% STMS solution,  $x$  being the final concentration of STMS in the HG, as schematically represented in Figure 1D. A picture of the obtained HGs is given in Figure 1E.

The impact of such STMS embedding in agarose HG in terms of mechanical properties was investigated by performing strain sweep measurements at a fixed frequency of 1 Hz and at 25 °C. The results, presented in Figure 2, confirm that the systems are in a hydrogel state, as the storage modulus  $G'$  remains higher

than the loss modulus  $G''$ . What can also be seen is that the addition of STMS increases the linear viscoelastic linear region of the hydrogel, without a clear impact of the amount of STMS though. However, increasing the amount of STMS clearly decreases the storage modulus  $G'$  from  $5711 \pm 613$  Pa (0 wt%) to  $3056 \pm 108$  Pa (5 wt%) but without affecting its gelation property.

We then investigated the loading and release of proteins, which was the main objective of this work. The basic procedure of the HG loading, in which conditions were established thanks

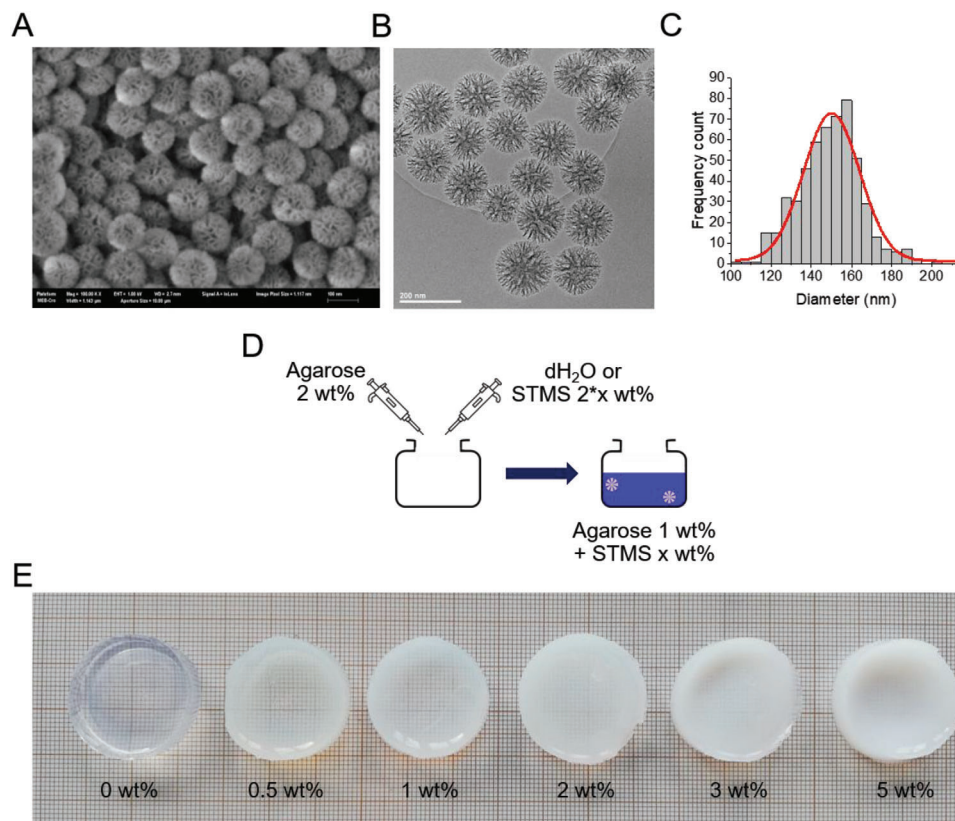


**Figure 1.** A) SEM image of the STMS NPs. B) TEM image of the STMS NPs. C) Size distribution of STMS NPs with the Gaussian fit of the curve. D) Schematic representation of the preparation of agarose/STMS composite HG. E) Picture of the obtained agarose/STMS composite HGs.

to preliminary experiments, is schematized in **Figure 3A**, and the loading results are shown in **Figure 3B**. As can be seen, the STMS loading contributes to increase the loading of HSA in the agarose/STMS composite HGs as the LC ranges from  $\approx 772 \pm 5 \mu\text{g mL}^{-1}$  (STMS free) to  $\approx 953 \pm 20 \mu\text{g mL}^{-1}$  (5 wt% STMS) which corresponds, respectively, to an LE ranging from  $\approx 77 \pm 0.5\%$  to  $\approx 95 \pm 2\%$ . These results correspond to the final loading, so taking into account the protein lost in the WS. But we quantified independently the LS and the WS to evaluate the amount of HSA that were just deposited on the surface of the HG and thus eliminated

by the quick washing. To do so, the  $m_{\text{loaded protein}}$  was evaluated using only the values measured in the LS and then the percentage of lost protein was expressed as a fraction of this loaded amount, as shown in Equation (3)

$$\text{Percentage of lost protein (\%)} = \frac{m_{\text{protein in WS}}}{2000 - m_{\text{protein in LS}}} \times 100 \quad (3)$$

with all the masses in  $\mu\text{g}$ .

The results presented in **Figure S2** (Supporting Information) indicate small losses for the STMS-free HG as  $\approx 4.7 \pm 0.2\%$  of the

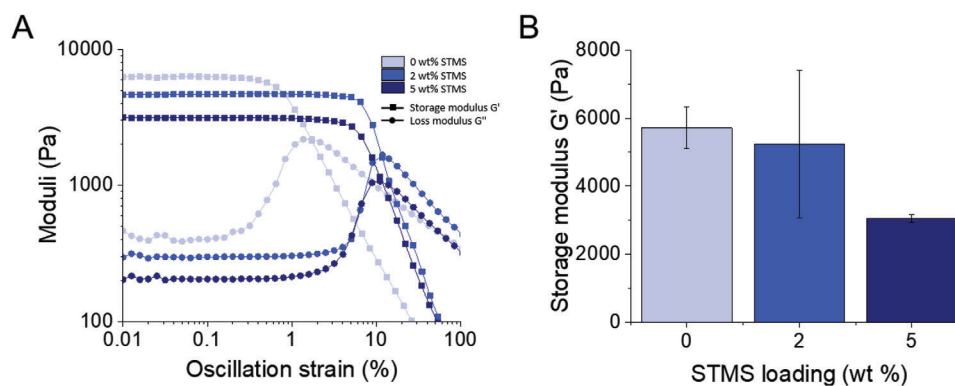


**Figure 2.** A) Representative curves of the storage and loss moduli evolution through strain sweep measurements for three agarose/STMS composite HGs. B) Evolution of the storage modulus  $G'$  in function of the amount of STMS.

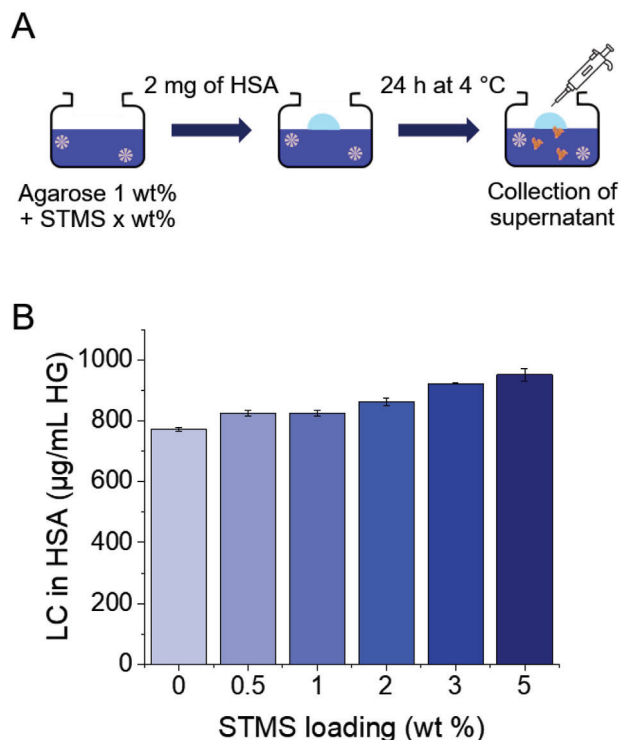


**Figure 3.** A) Schematic representation of the preparation of the agarose/STMS composite HG. B) LC of HSA in the HG in function of the amount of STMS.

total amount of loaded protein is lost during the washing. For the STMS-loaded HGs, the losses are still even lower (from  $\approx 3.8 \pm 0.4\%$  loss with 0.5 wt% of STMS to  $\approx 0.6 \pm 0.1\%$  loss with 5 wt%) meaning that the loading is very efficient with a good integration of almost all the HSA inside the agarose/STMS composite HGs.

We then studied the release of HSA from the agarose/STMS composite HGs over 144 h (6 days) and in  $\text{dH}_2\text{O}$ . We investigated this release at three different temperatures: 4 °C that would be a storage temperature, 37 °C that is the human biological temperature, and 45 °C that is a characteristic temperature in hyperthermia. We wanted to explore the release at this last temperature in addition to the others, as our team also has an expertise in the synthesis of iron oxide core@STMS shell nanoparticles (IO@STMS) that were already shown to be great heating agents under magnetic field stimulus and near infra-red light irradiation.<sup>[28,38,39]</sup> Such a study was then performed in order to evaluate the possible combination of protein release with magnetic or photonic hyperthermia, or even the improvement of protein release by hyperthermia. The release profiles of all the conditions are represented in **Figure 4**, and **Figure 5** regroups the release profiles at 37 °C for a better comparison. As it can be seen, the temperature did not impact significantly the release of HSA. However, and more importantly, the higher the STMS loading, the lower the HSA release, or the higher the HSA retention. Indeed, we decreased the HSA release from the totality (100%) without STMS to  $\approx 44 \pm 1.2\%$  with only 0.5 wt% of STMS and to  $\approx 1.4 \pm 0.9\%$  with 5 wt% of STMS.

From here, we considered our system as a protein retention system.

## 2.2. Versatility of the System toward Other Proteins

Following these very encouraging first results obtained with HSA, and with the aim to generalize this concept, we investigated the possibility of using agarose/STMS composite HGs for the retention of other proteins. Thus, we translated here the previous study to different proteins with a release performed in phosphate-buffered saline (PBS) at physiologic pH (7.4). We added HRP, ALP, and LYS to the study, where main characteristics are presented in **Figure 6A**, and we performed exactly the same experiments. The quantification technique used was still the BCA assay, with a calibration curve prepared for each protein in each solvent (see **Figures S3 and S4** in the Supporting Information for the calibration curves in  $\text{dH}_2\text{O}$  and in PBS, respectively). By doing so, we verified that there was no impact of the PBS buffer on the BCA assay. For all proteins used, and by increasing STMS amount from 0 to 5 wt%, the loading results (**Figure 6B**) gave similar trends than in the previous study, i.e., the protein loading was again improved by a higher amount of STMS. Further, the LE was again very high and improved as it ranged from  $\approx 77.1 \pm 0.6\%$  to  $\approx 94.8 \pm 0.7\%$  for HSA,  $\approx 77.1 \pm 0.6\%$  to  $\approx 99.3 \pm 0.2\%$  for HRP,  $\approx 77.3 \pm 1.2\%$  to  $\approx 80.8 \pm 2.2\%$  for ALP, and  $\approx 87.0 \pm 0.4\%$  to  $\approx 94.7 \pm 0.6\%$  for LYS. In addition, the loss during washing was also very low for all proteins (maximum  $\approx 5.4 \pm 0.2\%$ , which corresponds to HRP loaded in agarose HG with 0 wt% STMS) with again a strong reduction of this loss with the increase of the STMS amount (**Figure S5**, Supporting Information).

The protein release was also studied at the three temperatures with the same conditions used for HSA release over 144 h. For all the proteins, similar results than previously were obtained. First, the release profiles (**Figure 7**) show no impact of temperature increase on the release, except for ALP with a slight increase. More importantly, the comparison of the final release at 37 °C (**Figure 8**) also shows an increased retention of the proteins with the increase of the STMS loading as the protein release was reduced from  $\approx 99.2 \pm 5.2\%$  without STMS to  $\approx 45.1 \pm 2.1\%$  with only 0.5 wt% of STMS and  $\approx 9.4 \pm 7.2\%$  with 5 wt% of STMS in the case of HSA, which correlates well with the results obtained in  $\text{dH}_2\text{O}$ . Regarding the other proteins, the release dropped down from 100% for HRP and ALP to  $\approx 33.6 \pm 2.3\%$  (0.5 wt% STMS) and  $\approx 10.4 \pm 0.7\%$  (5 wt% STMS) in the case of HRP and to  $\approx 74.7 \pm 1.1\%$  (0.5 wt% STMS) and  $\approx 41.9 \pm 1.9\%$  (5 wt% STMS) in the case of ALP. The decrease of the release was even more impressive for LYS as it went from  $\approx 92.4 \pm 12.8\%$  (0 wt% STMS) to  $\approx 15.0 \pm 1.3\%$  (0.5 wt% STMS) and  $\approx 2.5 \pm 0.2\%$  (5 wt% STMS).

Thus, these experiments demonstrated i) the impressive loading efficiency of agarose/STMS composite HGs obtained with the four proteins, and ii) the clear retention of protein effect associated with the presence of STMS in the HG, which demonstrates the versatility of the approach toward various proteins.

## 2.3. Protein Retention Mechanism

As said in the “Introduction,” we used the STMS NPs expecting them to act as sub-micrometer size protein reservoirs embedded in the agarose HG. However, due to the temperature needed to prepare agarose HG ( $T > 80$  °C), it was impossible to directly embed protein-loaded STMS inside the HG, and we thus had to

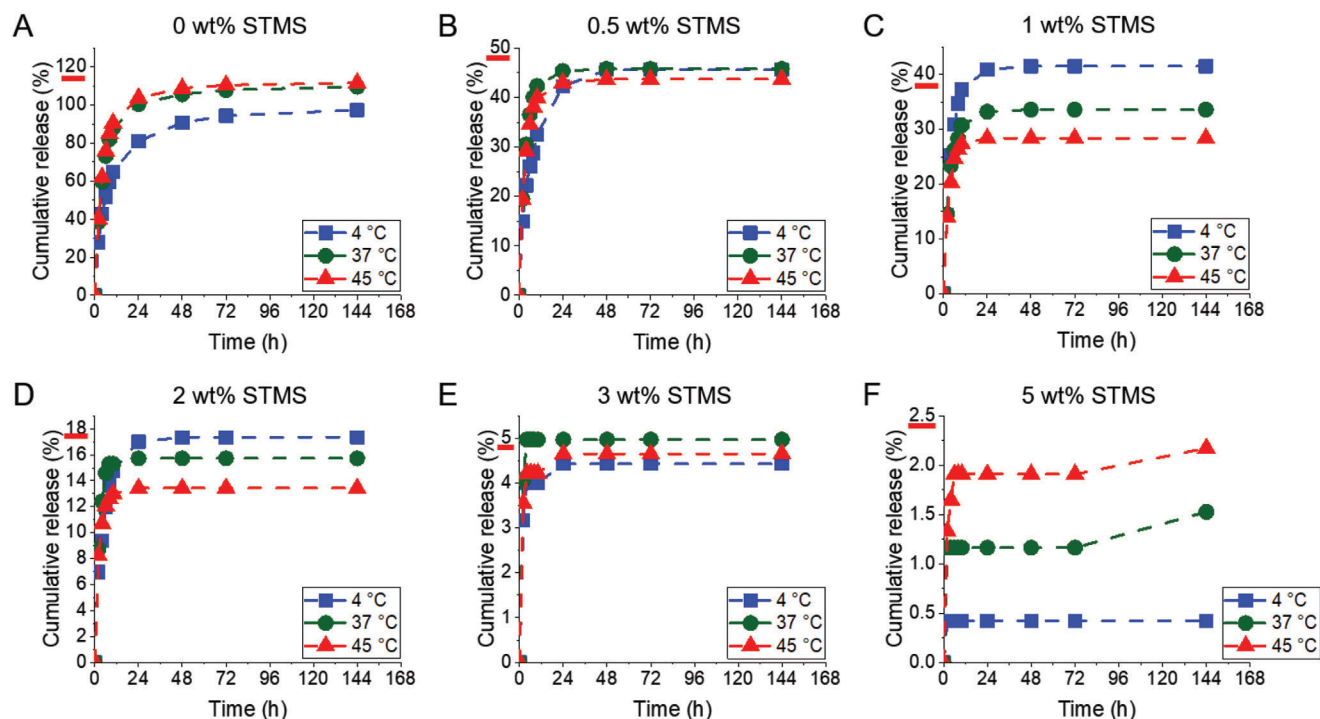


**Figure 4.** Release profiles at three temperatures of HSA when released from agarose/STMS composite HGs containing A) 0 wt%, B) 0.5 wt%, C) 1 wt%, D) 2 wt%, E) 3 wt%, and F) 5 wt% of STMS.

load the agarose/STMS composite HGs with proteins after fabricating them (postloading procedure). By doing so, we hypothesized that, following the protein addition and migration inside the agarose/STMS composite HG, the proteins were preferentially adsorbed to the embedded STMS. Hence, it was assumed that the proteins were stably immobilized on the STMS NPs and that only the remaining proteins loaded in the HG water pockets were released over the 144 h study, as schematized in **Scheme 2**. Thus, when there is enough STMS to “fix” all the proteins, we see a complete retention when performing the release study.

To validate our hypothesis that the proteins are specifically retained in the porous silica NPs, we used confocal microscopy and fluorescein isothiocyanate (FITC)/ Rhodamine B-isothiocyanate

(RITC)-labeled proteins to image their localization inside the nanocomposite HG. However, knowing that optical microscopy reaches at best  $\approx 300\text{--}400$  nm spatial resolution and that our

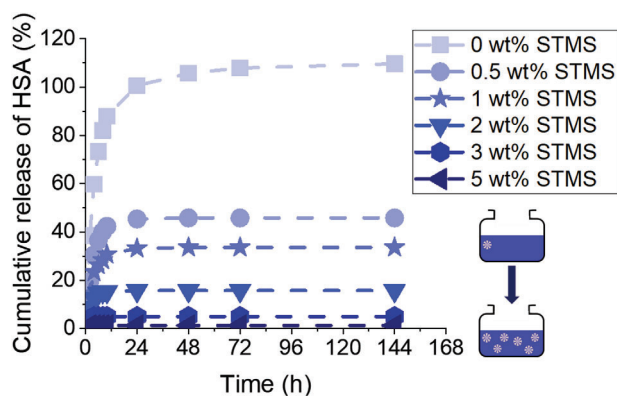


**Figure 5.** Release profile of HSA from different agarose/STMS composite HGs at 37 °C. PB.

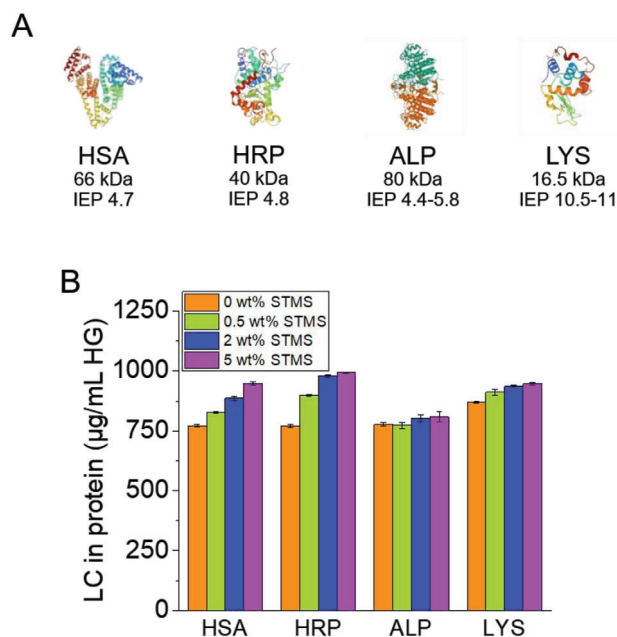


**Figure 6.** A) Representation of the four proteins of the study provided by Protein Data Base by Sugio et al.,<sup>[31]</sup> Berglund et al.,<sup>[32]</sup> Kim and Wyckoff,<sup>[33]</sup> and Muraki et al.,<sup>[34]</sup> respectively, together with their molecular weight and isoelectric point (IEP). B) LC obtained for the four proteins in different agarose/STMS composite HG.

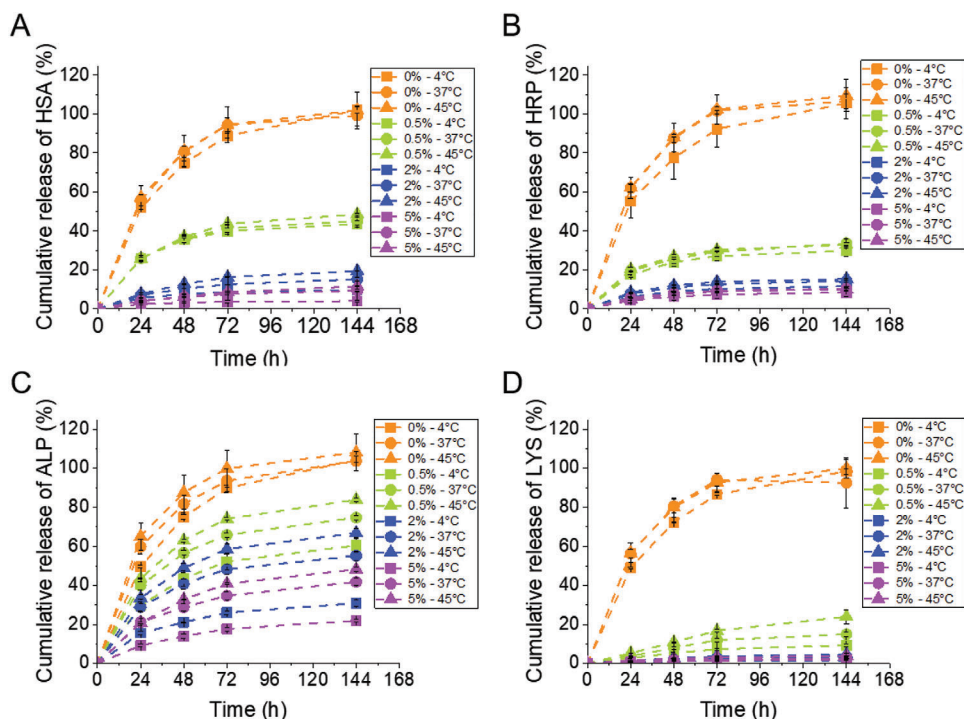


**Figure 7.** Release profiles at three temperatures of A) HSA, B) HRP, C) ALP, and D) LYS when released from an agarose/STMS composite HGs.

STMS has an average size of  $\approx 150 \pm 28$  nm, we needed thus to increase significantly the size of the silica particles in order to be able to visualize them individually inside the agarose HG. Thus, we synthesized bimodal silica microparticles (BMS) following the protocol first reported by Schulz-Ekloff et al.,<sup>[40]</sup> and with the separation technique described by Wang and Caruso.<sup>[41]</sup> We selected this protocol as it allows the synthesis of spherical silica particles of micrometric size and with pore sizes of 2–3 and 10–40 nm, which was good for us considering the pore size of  $\approx 15$

nm that we usually got with STMS.<sup>[28]</sup> Then, after their synthesis, the particles were characterized by scanning electron microscopy (SEM), TEM and nitrogen adsorption–desorption measurement, and results are shown in **Figure 9**. As it can be seen, we obtained particles with a size of  $1.61 \pm 0.64$   $\mu\text{m}$  with a Brunauer–Emmet–Teller (BET) surface of  $529 \text{ m}^2 \text{ g}^{-1}$  and representative mesopore sizes of  $\approx 4$  and  $\approx 13$  nm, which were suitable for our application.

Thus, we fabricated agarose/BMS composite HGs containing 0.5 wt% of BMS following the same protocol than for agarose/STMS composite HGs and we loaded them with HSA<sup>FITC</sup>, HRP<sup>FITC</sup>, ALP<sup>FITC</sup>, or LYS<sup>RITC</sup>. For each condition, we prepared an HG that was imaged right after loading and an HG from which we released the proteins for 48 h. The images presented in **Figure 10** (and taken in a representative interior section of the HG) show that, just after loading, we have the fluorescent proteins present on the HG part (background for HSA, HRP, and ALP) and on the BMS (co-localization between fluorescence and bright field images for all four proteins). After 48 h of protein release, these images show only a co-localization of FITC/RITC fluorescence with the BMS, which confirms the protein retention effect and that the released proteins were the ones present in the agarose HG part.

Regarding the fluorescence backgrounds (Figure 10, after loading), we can notice that the intensities are in the order ALP<sup>FITC</sup> > HSA<sup>FITC</sup> > HRP<sup>FITC</sup> > LYS<sup>RITC</sup>. Especially for LYS<sup>RITC</sup>, no fluorescence can be seen in the agarose part of the HG after loading, meaning that all the LYS<sup>RITC</sup> were fixed on the BMS. These results are in total agreement with the amount of released protein as shown in Figure 8; the addition of only 0.5 wt% of STMS corresponds to a protein spontaneous release of  $74.7 \pm 1.1\%$  (ALP<sup>FITC</sup>),  $45.1 \pm 2.1\%$  (HSA<sup>FITC</sup>),  $33.6 \pm 2.3\%$  (HRP<sup>FITC</sup>), and  $15.0 \pm 1.3\%$

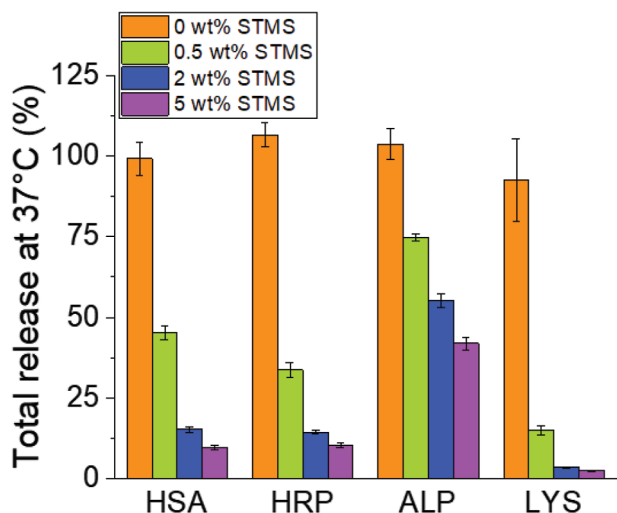
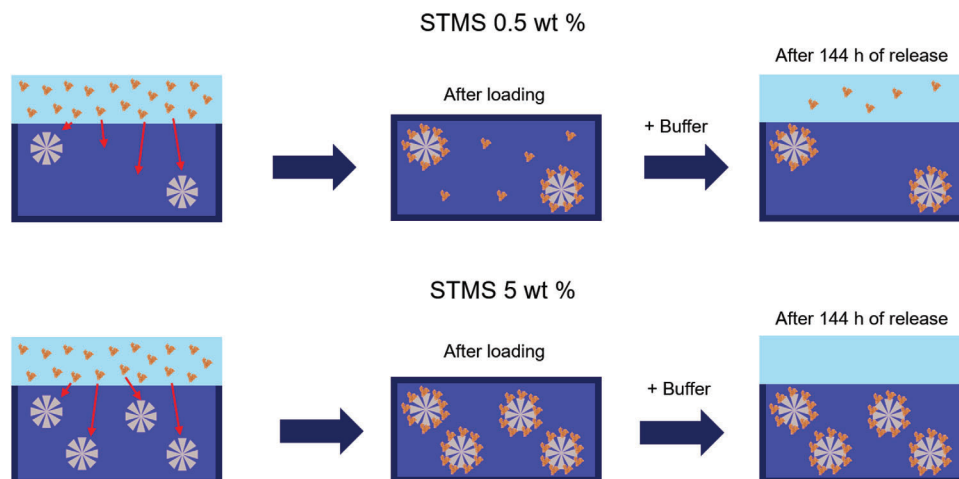


**Figure 8.** Final amount of released protein at 37 °C from the different agarose/STMS composite HGs.





**Scheme 2.** Schematic representation of the protein retention mechanism in the agarose/STMS composite HGs.

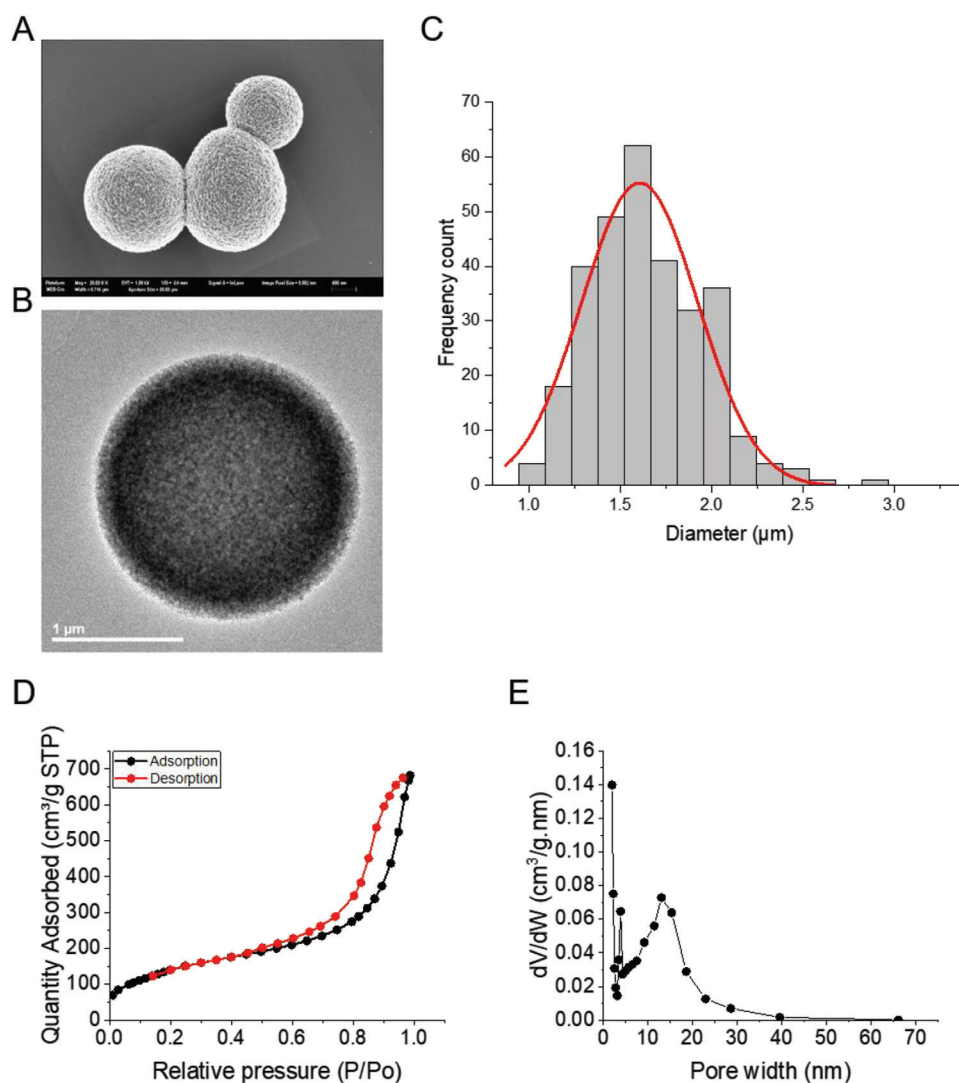


**Figure 9.** A) SEM and B) TEM images of the BMS microparticles. C) Size distribution of the BMS microparticles with the Gaussian fit curve (from SEM images). D) Nitrogen adsorption–desorption isotherm. E) BJH desorption pore volume plot.

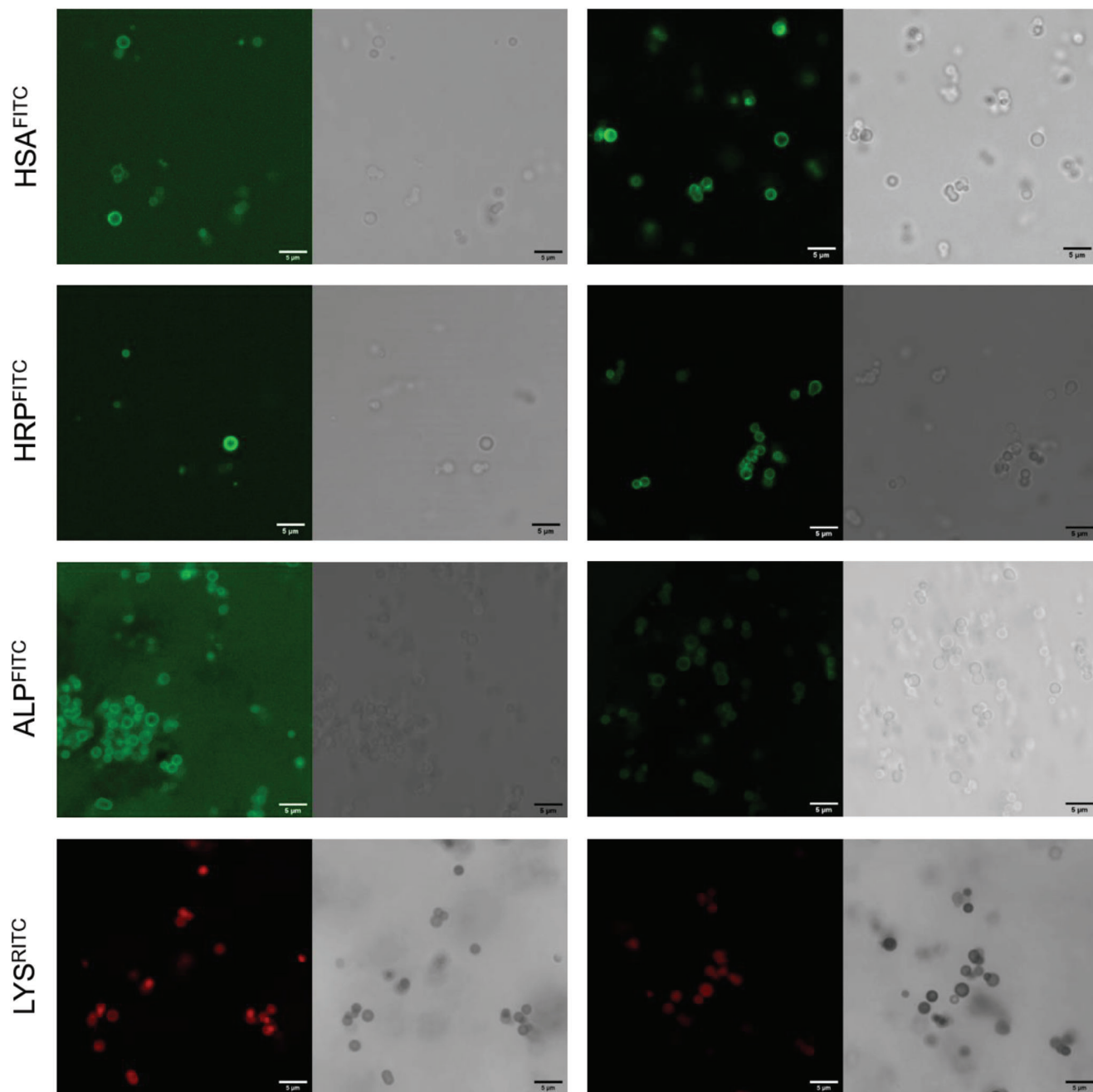


**Figure 10.** Confocal microscopy images (*xy* sections) of FITC/RITC-labeled protein-loaded agarose/BMS composite HGs after the loading and after 48 h of release.

(LYS<sup>RITC</sup>) for these four proteins. Here too for LYS<sup>RITC</sup>, this high reduction is then explained by the fact that in the HG, the LYS preferentially goes to the BMS even with a very low amount of particles. Such an increase of the LYS retention with a low amount of silica particles may come from higher affinity between LYS and silica surface than other proteins and silica surface. Strong electrostatic interactions are actually a possibility, as silica surface is negatively charged in dH<sub>2</sub>O and the isoelectric point (IEP) of LYS is 10.5–11, much higher than the ones of HSA, HRP, and ALP.

Further, the imaging of the total section of the HGs, from top to bottom, after 48 h of release (**Figure 11**) shows that this phenomenon is homogeneous in the whole agarose/BMS composite HG. This protein retention in BMS is really obvious for HSA<sup>FITC</sup>, HRP<sup>FITC</sup>, and LYS<sup>RITC</sup> while it is less marked for ALP<sup>FITC</sup>. It is important to notice that the case of ALP<sup>FITC</sup> was not that homogeneous. Indeed, as shown in Figure S6 (Supporting Information), we could observe that the BMS located at the top of the HG (which means the part that is in contact with the protein solution during the loading and with the buffer during the release) did not

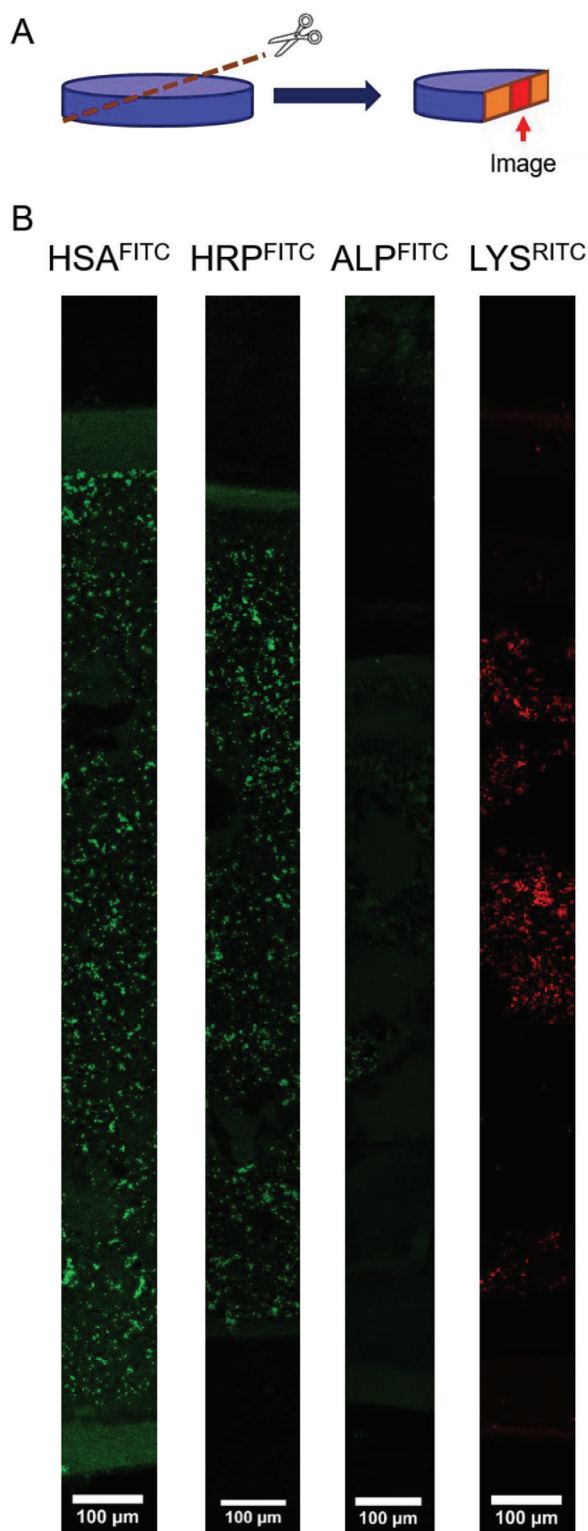


**Figure 11.** A) Schematic representation of the internal layer of agarose/BMS composite HGs imaged by confocal microscopy. B) Confocal microscopy images (*xz* sections) of the internal layer of FITC/RITC-labeled protein-loaded agarose/BMS composite HGs after 48 h of release.

display fluorescence: neither after the loading, nor after 48 h of release. This could come from a difference in the interactions at play between silica surface and ALP.

Finally, this confocal microscopy imaging experiment showed that the BMS act as retention systems inside the agarose HG by fixing the proteins and prevent their release, and that only the proteins present in the agarose part are then released.

We then wanted to see if these latter results could be extrapolated to our STMS NPs. In the first step, we evaluated the LCs in protein, referred to the STMS amount ( $\mu\text{g mg}^{-1}$ ) when the STMS are embedded in the HG. To do so, we considered that all the proteins that are in the agarose HG part were released after 144 h, which seems quite reliable regarding the release profiles shown in Figure 7, which then means that all the remaining proteins are adsorbed on the embedded STMS. This allowed us to calculate the LC in  $\mu\text{g}$  of protein per mg of STMS in the HGs. We then defined the feed weight ratio (FWR) in protein regarding the STMS amount as shown in Equation (4)

$$\text{FWR (\%)} = \frac{m_{\text{protein}}}{m_{\text{STMS}}} \times 100 \quad (4)$$

with all the masses in  $\mu\text{g}$ . We calculated that the HG containing 0.5 wt% of STMS corresponds to a FWR of 20% and that the HG containing 5 wt% of STMS corresponds to an FWR of 2%.

In the second step, we performed the adsorption of the four proteins on STMS dispersed in water ( $\text{dH}_2\text{O}$ ) with the same FWRs. We first started with the low FWR, as it corresponds to the HG containing 5 wt% of STMS, which seemed to be the best condition to adsorb proteins given the almost complete retention of proteins in the release study. The results gave a quite good correlation between the LC on STMS embedded in the HG and the LC on STMS dispersed in water (Figure 12A). The LCs are in the range of tens of  $\mu\text{g}$  of proteins per mg of STMS, but it is also interesting to give a look at the corresponding LE values (Figure 12B). Indeed, the LE was  $\approx 85.9 \pm 1.0\%$  for HSA,  $\approx 88.9 \pm 0.8\%$  for HRP, and  $\approx 92.3 \pm 0.6$  for LYS when STMS were embedded in an HG versus  $\approx 98.8 \pm 0.2\%$  for HSA and 100% for HRP and LYS when the STMS were dispersed in water. These values mean that there is a very good affinity between these three proteins and silica with no influence of the environment on the adsorption process. In the case of ALP, the LE values were  $\approx 52.8 \pm 2.9\%$  (in HG) and  $\approx 34.3 \pm 0.7\%$  (in water), showing a lower affinity with silica than the other proteins.

We then worked with an FWR of 20%, corresponding to an HG containing 0.5 wt% of STMS, to see how these values were affected by a change of FWR. The LC values were higher in this case (Figure 12C), as they ranged from  $\approx 36.4 \pm 6.0 \mu\text{g mg}^{-1}$  (ALP on STMS dispersed in water) to  $\approx 186.1 \pm 0.2 \mu\text{g mg}^{-1}$  (HRP on STMS dispersed in water). However, the correlation here was restricted to HSA and ALP, with notably a huge difference for LYS as its LC was  $\approx 154.8 \pm 3.3 \mu\text{g mg}^{-1}$  when STMS were embedded in the HG versus  $\approx 53.0 \pm 2.1 \mu\text{g mg}^{-1}$  when STMS were dispersed in water. These results show an influence of the environment on the global diffusion of proteins in the HG. Again, the LE values are very interesting (Figure 12D), especially if we compare them to the LE values obtained in the case of a low FWR. Indeed, the LE globally decreased with the increase of the FRW, meaning that in both HG and water, we reached the adsorption equilib-

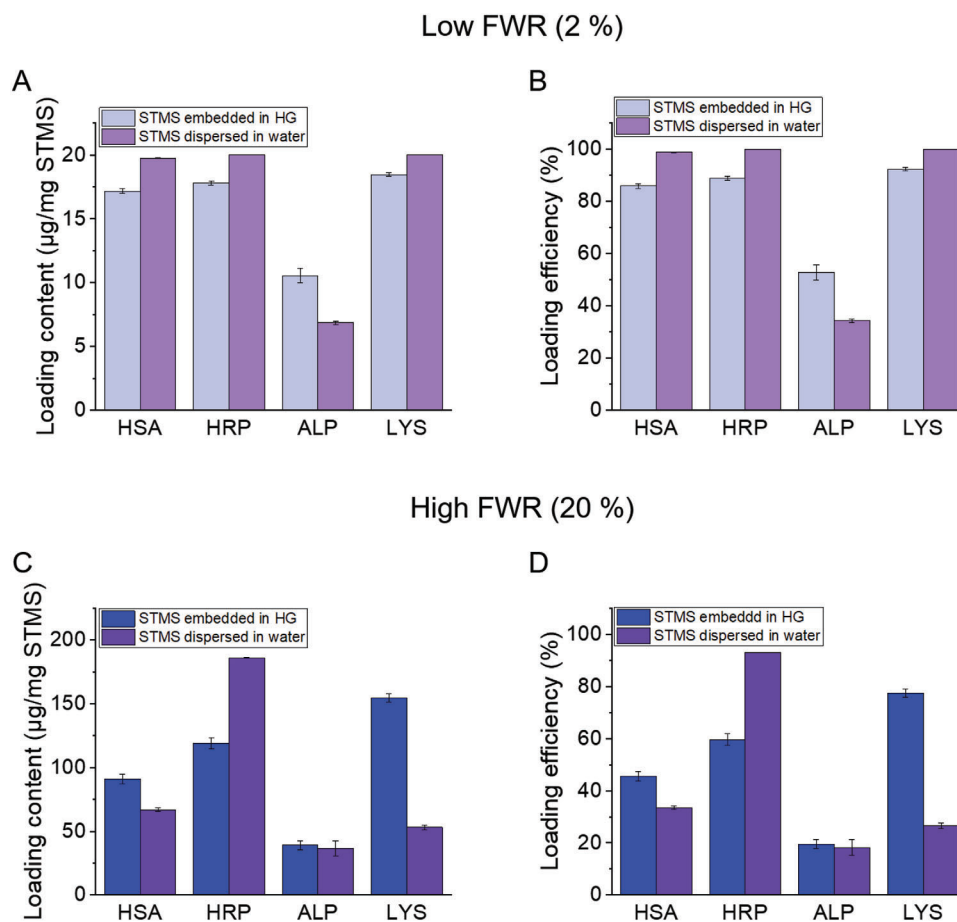


**Figure 12.** Comparative LC of protein regarding the STMS and LE when the NPs are embedded in an agarose HG or dispersed in water in the case A,B) of a low FWR and C,D) of a high FWR.

rium and got a fraction of proteins adsorbed on the STMS and a fraction of proteins dispersed in the environment. This result is in total agreement with the release profiles and results that we show in Figures 7 and 8 and with the confocal microscopy results. Even the still high LE obtained for LYS in an HG with a high FWR ( $\approx 77.4 \pm 1.7\%$ ) correlates well with the sharp decrease of the LYS release with only 0.5 wt% of STMS in the agarose HG and the absence of fluorescence background observed in the agarose/BMS composite HG after loading (Figure 10). In addition, the low LE obtained for ALP with both FWR values, together with the confocal microscopy observations, shows that the ALP does not adsorb with a very high efficiency on silica particles (BMS or STMS) whatever be the environment. As suggested after analyzing the confocal microscopy results, this difference could come from a difference of interaction between ALP and the silica surface compared to the other proteins and can explain the curve network shown in Figure 7C. Indeed, the LE obtained for ALP was almost the same whatever the environment or the FWR. This means that, unlike the other proteins, the increase of the STMS amount does not increase the amount of “fixed” ALP; thus, the retention is not really controlled by the amount of STMS and then we obtain the curve network as the fraction of adsorbed ALP on STMS and the fraction of ALP dispersed in the HG are not very different whatever the amount of STMS.

Regarding other proteins, all these results indicate that a low FWR in protein regarding the STMS amount may lead to a low LC, but to an LE of almost 100% and thus to an almost complete protein retention. In contrast, a high FWR will lead to a higher LC, but will reduce the LE, meaning that in the HG, the proteins will be partially adsorbed on the STMS and partially spread in the agarose HG part. This situation will then lead to an only partial retention of the proteins. In few words, controlling the FWR of protein regarding the STMS amount in an HG leads to the control of the protein retention inside the HG.

This experiment allows us to conclude that the protein adsorption occurs on the STMS embedded in the agarose HG in the same way than on the BMS embedded in the agarose HG. This confirms the protein retention mechanism by specific adsorption of proteins on the STMS NPs, that thus act as sub-micrometer size reservoirs in the HG.

## 2.4. Protein Structure and Biological Functions

### 2.4.1. Protein Conformation

In this section, we wanted to check the potential use of such nanocomposite HG to deliver active proteins. First, as it is well-

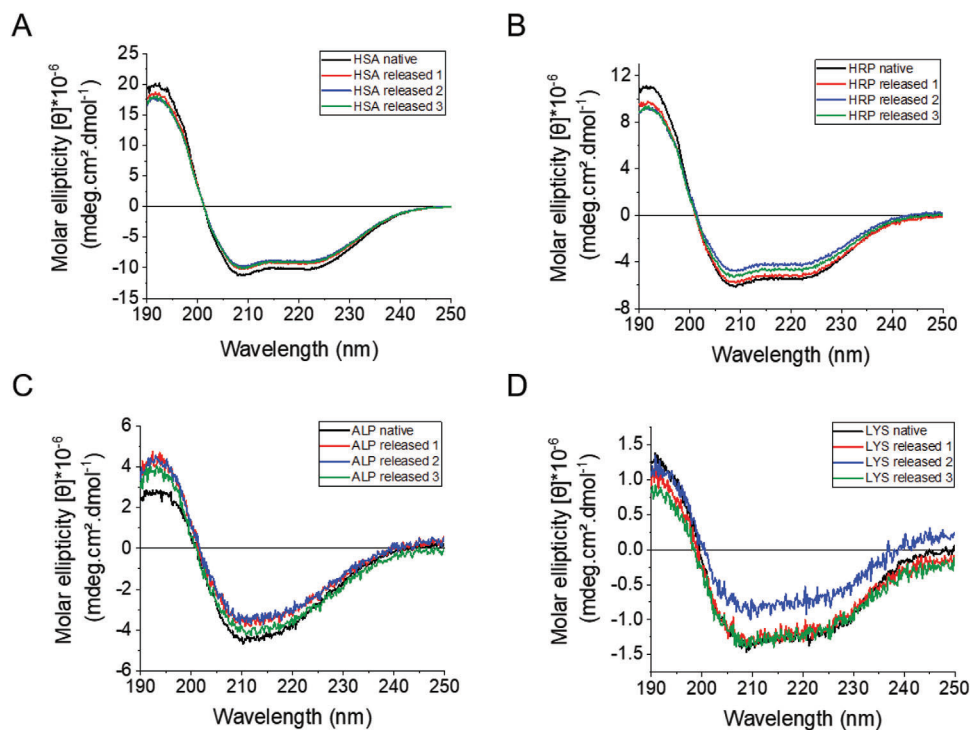


**Figure 13.** CD spectra of native and released proteins A) for HSA, B) for HRP, C) for ALP, and D) for LYS.

known that the conformation of proteins is an important parameter ensuring their biological activity, we investigated this characteristic by performing circular dichroism (CD) spectroscopy on the four native and released proteins. As we previously saw that the released proteins were the one located in the agarose part of the HG, we decided to perform this experiment using STMS-free HG, and to collect the released proteins after 24 h of release in triplicate from three similar HG samples. This allowed us to have enough proteins in our supernatant for the CD measurements and to check for potential changes from one HG to another. For this experiment, the release had to be performed in dH<sub>2</sub>O as PBS was found to absorb light below 200 nm ( $A > 2$ ), rendering this buffer unsuitable for such a measurement.

First of all, the measured ellipticity  $\theta$  was converted into molar ellipticity  $[\theta]$  using the following equation (Equation (5))

$$[\theta] \text{ (mdeg cm}^2 \text{ dmol}^{-1}\text{)} = \frac{\theta \times 10^6}{10 \times L \times C} \quad (5)$$

with  $\theta$  in mdeg,  $L$  the cuvette path length in cm, and  $C$  the protein concentration in  $\mu\text{mol L}^{-1}$ . Such a conversion was performed in order to normalize the curves and allow their comparison. As it can be seen in **Figure 13**, the CD spectra of released proteins have similar shapes as compared to the CD spectra of native ones for the four tested proteins. However, the intensity differs for most of them.

We then analyzed more in details these CD spectra by using the online program BestSel,<sup>[42–44]</sup> which allows the calculation of the secondary structure content (% of  $\alpha$ -helix, parallel and antiparallel  $\beta$ -sheets, turn and others). As can be seen in **Figure 14** (numerical values can be found in Tables S1–S4, Supporting

Information), some differences can be observed between native proteins and released proteins, but also between released proteins themselves. To give a short example, the proportion of antiparallel secondary structure increases between native HSA and released HSA, with a similar value for all released HSA. However, the proportion of these antiparallel secondary structures is different for all measured HRP.

This analysis shows that the process of loading and release of the proteins has an impact on their conformation. However, it is unsure that these changes detrimentally impact the biological activity of these proteins and thus prevent the use of such systems for medical application. Thus, we tested the enzymatic activity of two enzymes of our study: HRP and ALP.

#### 2.4.2. Enzymatic Activity of Released and Immobilized Proteins

Here, we wanted to check the activity of HRP and ALP on their well-known substrates. So, we used the ability of HRP to catalyze the oxidation of 2,2'-azino-bis(3-ethylbenzothiazoline-6-sulfonic acid) diammonium salt (ABTS) by H<sub>2</sub>O<sub>2</sub>, giving the radical cation ABTS<sup>•+</sup>, in which conversion can be followed by UV-visible spectroscopy at 420 nm, and the ability of ALP to hydrolyze 4-nitrophenyl phosphate disodium salt hexahydrate (pNPP-Na) into pNPP, where conversion can also be followed by UV-visible spectroscopy but at 405 nm. We considered two possibilities of performing these tests: either the protein would be released from the agarose HG, or the protein-loaded STMS NPs would be internalized by cells after degradation of the agarose HG. Thus, we performed the enzymatic activity on protein released by an STMS-free agarose HG and on protein immobilized on STMS

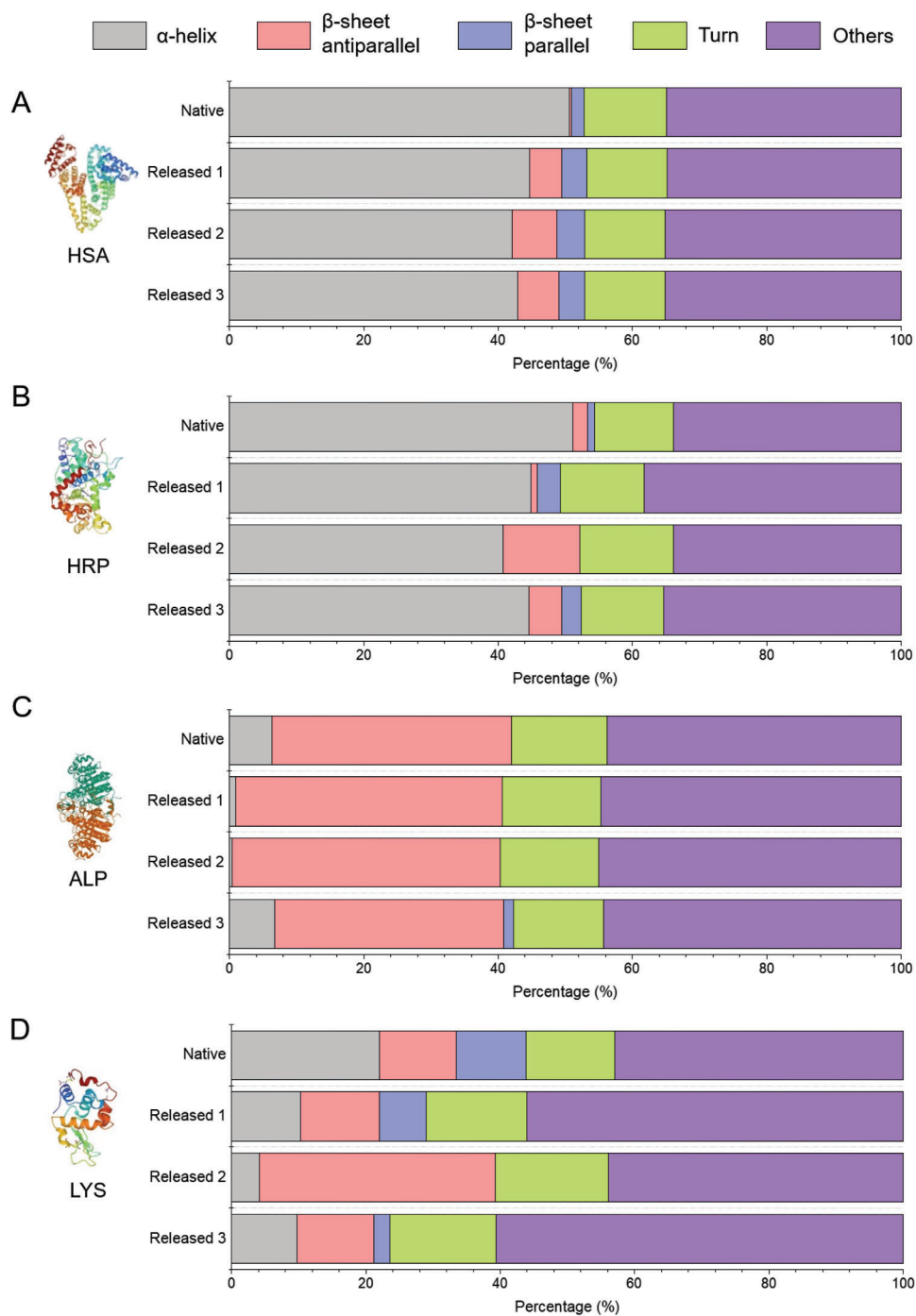


**Figure 14.** Secondary structure content obtained for A) HSA, B) HRP, C) ALP, and D) LYS.

NPs. In both cases, we also performed the test with the native protein solution to convert the absorbance value into relative activity. The results are given in **Figure 15** and show that the HRP is still very active whatever the situation. Regarding ALP, the activity is still very good when immobilized on STMS NPs but is reduced when the ALP is released from an agarose HG. However, we can see that the relative activity is increasing with time so the protein still has a good activity.

So, we could show here that the proteins were still active whatever they were released directly from the HG or immobilized on STMS.

### 3. Conclusion

In this work, we have investigated the properties of a new kind of PDS consisting in a nanocomposite HG formed from large pore

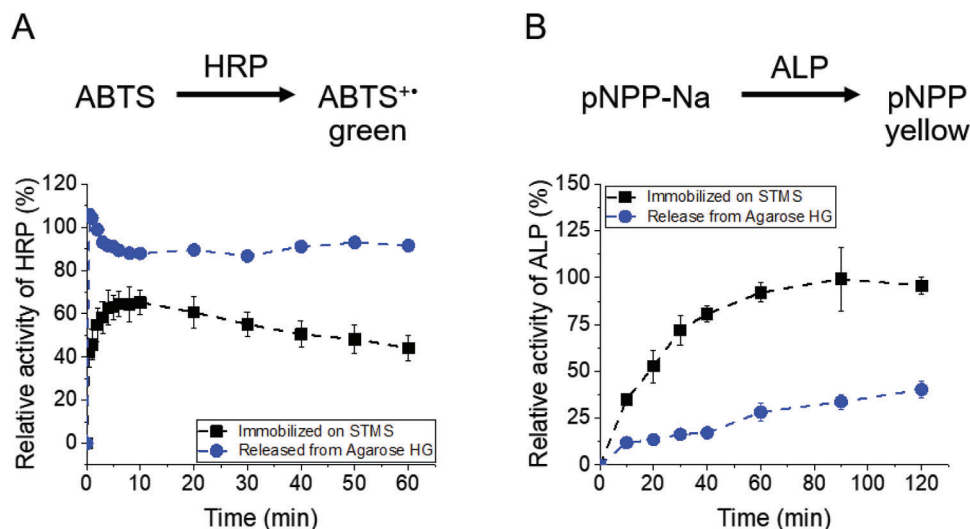


**Figure 15.** Relative enzymatic activity of A) HRP and B) ALP when they are immobilized on STMS NPs or released from an agarose HG.

STMS NPs embedded in an agarose HG. The main properties of such a system are summarized as follows:

- i. By using HSA as a model protein, the protein burst release and the protein retention in the HG could be efficiently and simply tuned by playing on the NPs amount dispersed within the HG. For instance, the spontaneous protein release collapsed from 100% without any loaded particles up to 1% when the HG was loaded with 5 wt% of STMS, indicating the powerful retention effect of the NPs.
- ii. By applying this study to the three other proteins HRP, ALP, and LYS that notably are enzymes and importantly are of different hydrodynamic sizes and IEPs, we showed the versatility of this behavior toward various proteins.
- iii. The mechanism of the protein retention was demonstrated by confocal microscopy using micrometer-sized BMS particles. Data showed that the porous silica particles act as protein reservoirs retaining the proteins while spontaneous release was attributed to proteins diffusing from the HG water pockets of the agarose HG. This mechanism could be extrapolated to the agarose/STMS composite HG by comparing the loading of protein regarding the STMS amount when the NPs were embedded in the HG or dispersed in water.
- iv. Even if the CD spectroscopy showed a change of the secondary structure content between native and released proteins, the biological activities of HRP and ALP enzymes were validated whether they were released over 144 h from an STMS-free agarose HG or immobilized on STMS NPs. This showed that the enzymes would still be active whether they are released from the water pockets of the agarose HG or internalized by cells in the form of adsorbed protein on STMS NPs due to cell-induced agarose HG degradation.

Due to the ease of fabrication of this system and its versatility toward various proteins, it could be envisioned to use it as a platform composite HG that could be stored and loaded with the desired protein only when the time requires it.

## 4. Experimental Section

**Materials:** The materials were used as provided. Cetyltrimethylammonium *p*-toluene sulfonate (CTATos, CAS 138-32-9), Trizma base (AHMPD, CAS 77-86-1), HSA (66 478 g mol<sup>-1</sup>, CAS 70024-90-7), and RITC (CAS 36877-69-7) were purchased from Sigma life science. Peroxidase from horseradish (40 000 g mol<sup>-1</sup>, ≈150 U mg<sup>-1</sup>, CAS 9003-99-0), Lysozyme from human (16 500 g mol<sup>-1</sup>, CAS 12671-19-1), and phosphate-buffered saline (PBS) were purchased from Sigma. ABTS (CAS 30931-67-0), pNPP-Na (CAS 4264-83-9), and (1-hexadecyltrimethyl) ammonium bromide (CTAB, CAS 57-09-0) were purchased from Alfa Aesar. Sodium carbonate (NaHCO<sub>3</sub>, CAS 144-55-8) and ALP (80 000 g mol<sup>-1</sup>, CAS 9001-78-9) were purchased from Sigma–Aldrich. Dimethyl sulfoxide (DMSO, CAS 67-68-5) and ethyl acetate (C<sub>4</sub>H<sub>8</sub>O<sub>2</sub>, CAS 141-78-6) were purchased from Roth. Hydrogen peroxide 35% (H<sub>2</sub>O<sub>2</sub>, CAS 7722-84-1) was purchased from Acros Organics, tetraethylorthosilicate (TEOS, CAS 78-10-4) from Aldrich chemistry, anhydrous absolute ethanol (EtOH, CAS 64-17-5) from Carlo Erba Reagents, QA-agarose multipurpose (MW ND, 9012-36-6) from MP Biomedicals, metasilicate de sodium anhydre (Na<sub>2</sub>SiO<sub>3</sub>, CAS 6834-92-0) from Fluka, FITC (CAS 3326-32-7) from TCI and the MicroTM protein assay kit from ThermoScientific.

**Synthesis of Silica Particles:** Synthesis of STMS. For the synthesis of STMS, the protocol was used as described previously.<sup>[29,35–37]</sup> A 500 mL flask was used for the reaction in which CTATos (3.8 g), AHMPD (0.436 g), and 200 mL of dH<sub>2</sub>O were introduced and stirred at 75 °C up to full dissolution (about 30 min). The TEOS was then added (30.2 g) prior to leave the reaction under stirring for 2 h at 75 °C. After 2 h, a white precipitate could be observed and the mixture was cooled before being transferred into 50 mL centrifugation tubes and centrifuged (13,000 g, 20 min). The precipitates were then collected and the CTATos was eliminated by a calcination step of 10 h at 550 °C. The final amount of powder was generally between 4 and 5 g. The resuspension of the STMS was done first by using a mortar to crush the white powder into a fine powder. This fine powder was then transferred in a 50 mL tube and resuspended in 20 mL of EtOH using the sonication bath for 30 min and regularly the vortex. The residual aggregates were then eliminated with a fast centrifugation cycle (30 s with the centrifuged programmed for 10 min at 11 000 G). The supernatant was transferred to a new tube, and the concentration was evaluated by drying and weighting a known volume of the solution. The tube was stored on a wheel until use.

Synthesis of BMS. The synthesis of BMS particles was performed according to the protocol reported by Schulz-Ekloff et al.,<sup>[40]</sup> and adapted by Wang and Caruso.<sup>[41]</sup> The CTAB (9.8 g) and Na<sub>2</sub>SiO<sub>3</sub> (5 g) were added to a

500 mL flask with 175 mL of dH<sub>2</sub>O and dissolved under magnetic stirring at 30 °C. Then, a volume of 17.5 mL of ethyl acetate was added and the mixture was stirred for 30 s. The flask was then removed from the oil bath and the mixture was left to age for 5 h at an ambient temperature (21 °C). After this ageing time, the flask was put back in the oil bath at 90 °C, and the reaction was performed 48 h under magnetic stirring. The BMS were collected by multiple sedimentation steps in 50 mL centrifugation tubes. Basically, the solution was transferred to four tubes and left to sediment for 5 min. The supernatant was then collected with a 10 mL pipette and transferred to new tubes. The sedimentation was repeated five times. The particles were then washed twice with 20 mL of EtOH (centrifugation step: 5 min, 1000 g). The organic materials were eliminated by calcination (10 h at 600 °C).

**Fabrication of Agarose/Particles Composite HGs:** The protocol here is described for the preparation of four HGs at 1 wt% of agarose and 0.5 wt% of STMS. The HGs were prepared in 12.5 mL glass vials (neck diameter = 30 mm). First, the 20 mg mL<sup>-1</sup> agarose stock solution was prepared by dissolving 100 mg of agarose in 5 mL of dH<sub>2</sub>O in a 50 mL centrifugation tube. The tube was then placed in an oven at 80 °C and manually shaken regularly until the agarose was dissolved. In parallel, the adequate volume of STMS NPs stock solution was collected in order to have 45 mg of STMS. The particles were then washed three times with dH<sub>2</sub>O (centrifugation 10 min, 13 000 g) and resuspended in 4.5 mL of dH<sub>2</sub>O in order to have 10 mg mL<sup>-1</sup>.

To prepare the HGs, 1 mL of the STMS solution was transferred in the glass vial and placed in the oven at 80 °C. A volume of 1 mL of agarose was then added and the solution was mixed up and down with a paster pipette. The glass vial was then removed from the oven, closed, and placed in the fridge once the HGs were formed (10 min later). The final HGs were kept at 4 °C prior to be used between 1 h and 3 days.

**Labeling of Proteins:** HSA, HRP, and ALP were labeled with FITC using a molar ratio of two FITC for one protein and the solutions were protected from light during all the procedure. Basically, 50 mg of protein was dissolved in 5 mL of NaHCO<sub>3</sub> buffer (0.1 mol L<sup>-1</sup>, pH 8.5) to obtain a 10 mg mL<sup>-1</sup> solution. Then, the adequate volume of 10 mg mL<sup>-1</sup> solution of FITC in DMSO was added, and the solution was stirred for 1 h. The solution was then dialyzed for 2 days in dH<sub>2</sub>O to remove the free FITC with a change of water every 2 h. Finally, the solution was collected and the final volume measured to calculate the exact concentration taking into consideration the swelling of the dialysis bag. The solution was then stored at -20 °C.

LYS was labeled with RITC using a molar ratio of one RITC for one LYS. Here also, the solution was protected from light during all the procedure. The general protocol was the same except that the protein and the RITC were dissolved in PBS at pH 8.4 and that the RITC concentration was 2 mg mL<sup>-1</sup>.

**Loading of HGs or STMS with Proteins:** Loading of HG. The loading process of HG with proteins was the same for unlabeled and labeled proteins except that the vials were protected from light when using labeled proteins. Briefly, it was decided to use 2 mg of proteins added in 200 µL for 2 mL of HG. Thus, a stock solution of 10 mg mL<sup>-1</sup> of protein in dH<sub>2</sub>O was prepared, and 200 µL was added on the HG. The vial was closed with the cap and placed at 4 °C for 24 h. Then, the 200 µL of supernatant was collected and the HG was washed with 1 mL of dH<sub>2</sub>O. This washing supernatant was also collected.

Loading of STMS. In case of loading of STMS with proteins, the adsorption was done in triplicate for the four proteins and at the same time for all the proteins. Thus, the adequate volume of STMS was collected in order to get 48 mg, and was washed three times with 10 mL of dH<sub>2</sub>O (centrifugation 11 000 × g, 10 min) prior to be resuspended in 24 mL of dH<sub>2</sub>O (2 mg mL<sup>-1</sup>). A volume of 1 mL of the solution (2 mg) was then collected and transferred to 1.5 mL tubes prior to be centrifuged (11 000 × g, 10 min) and resuspended in 50 µL of dH<sub>2</sub>O. Then a volume of 500 µL of protein stock solution at 0.8 or 0.008 mg mL<sup>-1</sup> was added to the tubes (feed weight ratio in protein of 20% and 2%, respectively). The solutions were homogenized with the vortex and mixed for 1 h on the wheel. The NPs were then centrifuged (11 000 × g, 10 min) and the loading supernatant collected for quantification.

**Release of Proteins:** To release the proteins, 2 mL of buffer (dH<sub>2</sub>O or PBS pH 7.4) was added on the HG in the vials. The vials were closed and placed in the fridge at 4 °C or in an oven at 37 or 45 °C with a tube of the buffer. The 2 mL supernatant was collected and replaced by fresh buffer at the corresponding temperature at each time point. The supernatants were kept at 4 °C prior to be used for quantification.

**Enzymatic Activity:** The enzymatic activity was performed on HRP and ALP immobilized on STMS and released by an agarose HG (0 wt% of STMS) after 144 h. The control was performed using the protein solution that was used to load the HG in order to have the same age of the solution. In addition, the control corresponding to the protein released by an HG was prepared with the same amount of PBS to be in the exact same buffer.

**HRP enzymatic activity.** The enzymatic activity of HRP was evaluated in dH<sub>2</sub>O by checking its ability to catalyze the oxidation of ABTS substrate by H<sub>2</sub>O<sub>2</sub>. The oxidation of ABTS was monitored by recording UV-vis spectra between 415 and 425 nm. The results were plotted using the maximum absorption at 420 nm. In a general procedure, 0.5 mL of the HRP solution was prepared and quickly mixed with 0.5 mL of an ABTS solution (0.2 mg mL<sup>-1</sup>). The solution was then transferred into a 1 cm path length beveled plastic cuvette (1 mL capacity) that was positioned in the UV-visible spectrometer. A volume of 2 µL of H<sub>2</sub>O<sub>2</sub> (350 mg mL<sup>-1</sup>) was then added and the chronometer started. The absorbance was measured at 30 s and 1–2–3–4–5–6–8–10–20–30–40–50–60 min.

An amount of 125 µg of STMS@HRP was used for the assay, which represented a quantity of 23.3 µg of HRP. The same amount was then used for the control.

The concentration of HRP in the supernatant "144 h" was measured to be 41.17 µg mL<sup>-1</sup> and a volume of 500 µL of this solution was used for the assay, corresponding to 20.585 µg of HRP in 500 µL of PBS. The HRP stock solution was at 10 mg mL<sup>-1</sup> in dH<sub>2</sub>O. Thus, the control was prepared by diluting 4.117 µL of the HRP stock solution in a final volume of 1 mL of PBS. The volume of dH<sub>2</sub>O was considered to be negligible.

**ALP enzymatic activity.** The enzymatic activity of ALP was evaluated in NaHCO<sub>3</sub> (50 mmol L<sup>-1</sup>, pH 8.5) by checking its ability to convert pNPP-Na to pNPP. The conversion of pNPP-Na was monitored by recording UV-vis spectra between 400 and 410 nm. The results were plotted using the maximum absorption at 405 nm. In a general procedure, 1 mL of ALP solution was mixed with 1 mL of pNPP-Na (0.1 mg mL<sup>-1</sup>) in a 5 mL centrifugation tube. The tube was then covered with aluminum and kept at 37 °C with a water bath. The absorbance was measured at 10–20–30–40–50–60–90, and 120 min.

An amount of 0.5 mg of STMS@ALP was used for the assay, which represented a quantity of 23.3 µg of ALP. The same amount was then used for the control.

The concentration of ALP in the supernatant "144 h" was measured to be 70.48 µg mL<sup>-1</sup>. A volume of 1 mL at 20 µg mL<sup>-1</sup> in NaHCO<sub>3</sub> buffer was prepared by diluting 284 µL of this supernatant that was in PBS. The control was prepared by first preparing a solution at 70.48 µg mL<sup>-1</sup> in PBS with the ALP stock solution and then by preparing 1 mL at 20 µg mL<sup>-1</sup> in NaHCO<sub>3</sub> buffer using the same dilution than for the supernatant. Thus, the quantity of PBS was the same in the sample and in the control.

**Characterization Methods:** Dynamic light scattering (DLS). DLS measurements were recorded in triplicate at 25 °C and at a scattering angle of 173 ° using a 1 cm path length plastic cell and a Zetasizer Nano-ZS (Malvern instruments). The measurements were conducted to check the good dispersivity of STMS NPs after resuspension in EtOH.

Transmission electron microscopy (TEM). TEM images were acquired with a JEOL 2100 TEM instrument operating at 200 kV after depositing the STMS on carbon-coated copper grids. The size distribution of STMS was then determined using the software Image J.

Scanning electron microscopy (SEM). SEM images were acquired with a Gemini SEM 500 microscope equipped with a field emission gun (SEM-FEG) and operating at 1 kV. The InLens signal, using secondary electrons, was used to get the images. The sample was prepared by depositing one drop of the BMS in EtOH on a silicium wafer. After evaporation of the solvent, the sample was coated with 10 nm of carbon.

Rheology. The rheological measurements were performed on a Discovery Hybrid Rheometer HR-3 from Waters/TA Instruments using a Peltier



plate geometry and an upper parallel plate with a diameter of 25 mm. Strain sweep tests were performed from 0.01% to 100% at a fixed frequency of 1 Hz at 25 °C. The gap was set around 2.4 mm and adjusted for each HG. To ensure proper measurements, 3 mL of HGs was prepared in small Petri dish (diameter 35 mm), and a round cutter with a diameter of 25 mm was used to obtain the right HG diameter. Each type of HG (0–2–5 wt% STMS) was tested in triplicate.

**Nitrogen adsorption.** N<sub>2</sub> adsorption–desorption measurements at –196 °C were performed in order to obtain the specific surface area and the pore size of the particles. To do so, the BMS were degassed under vacuum at ambient temperature (around 20 °C) for 3 h to desorb the moisture before analysis. The BET method was used to calculate the specific surface area and the Barrett–Joyner–Halenda (BJH) method was used to determine the pore volume and pore size distribution using the desorption branch. Finally, the Horvath–Kawazoe model was used to determine the pore size distribution in a micropore analysis from a single adsorption isotherm (dosing of nitrogen = 2 cm<sup>3</sup>, stability time = 3 h).

**Bicinchoninic Acid assay (BCA).** The BCA assay relies on the reactivity of the peptide bonds in proteins toward copper ions. Indeed, the peptide bonds are able to reduce Cu<sup>2+</sup> into Cu<sup>+</sup>, which then forms a purple metallic complex with two BCA molecules, making it detectable by UV–vis spectroscopy.<sup>[45,46]</sup> The BCA test was conducted using a BCA kit from ThermoFisher. In a typical procedure, a calibration curve was prepared for each protein with a volume of 500 µL for each point in dH<sub>2</sub>O or in PBS in 1.5 mL tube. Then, the supernatants were diluted adequately in a final volume of 500 µL in 1.5 mL tube. The provider's protocol was followed to prepare the BCA reactive solution by mixing solutions A (tartrate–carbonate alkaline buffer), B (bicinchoninic acid solution), and C (copper sulfate solution) in the proportion of 50%, 48%, and 2% respectively. Then, 500 µL of the BCA reactive solution was added to each tube. The tubes were vortexed and incubated for 1 h at 60 °C. The solutions were then cooled to room temperature using a water bath and the UV–vis absorbance was measured between 560 and 570 nm. The value at 562 nm was used for the quantification. Based on the difficulty to quantify proteins studied in a previous paper,<sup>[29]</sup> in the literature and experimentally, a calibration curve was performed for each protein in each solvent. The minimal concentration of protein reliably detected by these assays was determined to be 1 µg mL<sup>–1</sup> for HSA from previous experiments. A concentration as low as 1.25 µg mL<sup>–1</sup> was determined for HRP, ALP, and LYS with no need to check for lower detectable concentration.

**UV-visible spectroscopy.** UV–vis spectroscopy was performed on a Lambda 950 UV/Vis spectrometer (PerkinElmer precisely) with 1 cm path length plastic cell (beveled or not depending the experiment).

**Confocal laser scanning microscopy.** Confocal laser scanning microscopy images were captured with a Zeiss LSM 710 microscope (Carl Zeiss, Germany) using a x63 PLAPO (1.4 Numerical Aperture). The fluorescence of fluorescein was measured with an excitation wavelength of 488 nm and an emission wavelength between 596 and 540 nm, and the fluorescence of RITC was measured with an excitation wavelength of 561 nm and an emission wavelength between 566 and 703 nm.

**Circular dichroism (CD).** CD spectra were recorded on a J-1700 CD spectrometer (Jasco) using a 1 cm path length quartz cell with low intrinsic CD (Starna). An accumulation of 3 spectra was performed, collected from 250 to 190 nm with a step of 0.2 nm, a bandwidth of 0.5 nm, a scanning speed of 5 nm min<sup>–1</sup>, and a digital integration time of 2 s. Due to absorbance of PBS below 200 nm, all the measurements were performed in dH<sub>2</sub>O.

The native proteins were diluted to 0.5 µmol L<sup>–1</sup> for HSA, HRP, and LYS, and to 0.25 µmol L<sup>–1</sup> for ALP in order to avoid signal saturation according to preliminary measurements. The released proteins were collected after loading and 24 h release from STMS-free HG using dH<sub>2</sub>O as the releasing solvent, and further diluted to ≈0.4 µmol L<sup>–1</sup> for HSA, HRP, and LYS and to 0.15 µmol L<sup>–1</sup> for ALP. The calculation for such dilutions was based on the release studies and the targeted concentrations were lowered to be sure not to saturate the signal on the CD apparatus. The exact concentrations were quantified afterward using the BCA assay.

**CD curve processing.** A conversion of the signal from the ellipticity  $\theta$  to molar ellipticity  $[\theta]$  was performed using the following equation (Equa-

tion (5)) in order to normalize the signal, and allowing a better comparison of the curves

$$[\theta] \left( \text{mdeg cm}^2 \text{ dmol}^{-1} \right) = \frac{\theta \times 10^6}{10 \times L \times C} \quad (6)$$

with  $\theta$  in mdeg,  $L$  being the cuvette path length in cm, and  $C$  be the protein concentration in µmol L<sup>–1</sup>.

The CD spectra were then analyzed with the online program BestSel considering that HSA, HRP, ALP, and LYS contain 585,<sup>[47–49]</sup> 308,<sup>[50,51]</sup> 1028,<sup>[52–54]</sup> and 130<sup>[55–57]</sup> residues, respectively.

## Supporting Information

Supporting Information is available from the Wiley Online Library or from the author.

## Acknowledgements

D.M. and J.B. acknowledge the Agence Nationale de la Recherche (Grant No. ANR-19-CE09-0004—Corelmag) for financial supports. The spectroscopy and the transmission electronic microscopy platforms of the IPCMS and the characterization platform of ICPEES are acknowledged for technical supports. Dr. M. Pauly, S. Veyzalova, and C. Mélat are greatly thanked for fruitful discussions and technical supports.

## Conflict of Interest

The authors declare no conflict of interest.

## Data Availability Statement

The data that support the findings of this study are available from the corresponding author upon reasonable request.

## Keywords

biocatalytic materials, nanocomposite hydrogel, protein release, protein reservoirs, stellate mesoporous silica

Received: March 14, 2024

Revised: March 25, 2024

Published online:

- [1] J. Bizeau, D. Mertz, *Adv. Colloid Interface Sci.* **2021**, *287*, 102334.
- [2] B. Leader, Q. J. Baca, D. E. Golan, *Nat. Rev. Drug Discovery* **2008**, *7*, 21.
- [3] M. Yu, J. Wu, J. Shi, O. C. Farokhzad, *J. Controlled Release* **2016**, *240*, 24.
- [4] S. D. Putney, P. A. Burke, *Nat. Biotechnol.* **1998**, *16*, 153.
- [5] B. S. McAvan, M. Khuphe, P. D. Thornton, *Eur. Polym. J.* **2017**, *87*, 468.
- [6] X. Qi, W. Wei, J. Li, G. Zuo, X. Pan, T. Su, J. Zhang, W. Dong, *Mol. Pharmaceutics* **2017**, *14*, 431.
- [7] D. S. Lima, E. T. Tenório-Neto, M. K. Lima-Tenório, M. R. Guilherme, D. B. Scariot, C. V. Nakamura, E. C. Muniz, A. F. Rubira, *J. Mol. Liq.* **2018**, *262*, 29.
- [8] X. Ma, T. Xu, W. Chen, H. Qin, B. Chi, Z. Ye, *Carbohydr. Polym.* **2018**, *179*, 100.

- [9] L. Dai, T. Cheng, Y. Wang, H. Lu, S. Nie, H. He, C. Duan, Y. Ni, *Cellulose* **2019**, 26, 6891.
- [10] M. G. L. Olthof, D. H. R. Kempen, X. Liu, M. Dadsetan, M. A. Tryfonidou, M. J. Yaszemski, W. J. A. Dhert, L. Lu, *J. Tissue Eng. Regen. Med.* **2018**, 12, 1339.
- [11] W. Wei, J. Li, X. Qi, Y. Zhong, G. Zuo, X. Pan, T. Su, J. Zhang, W. Dong, *Carbohydr. Polym.* **2017**, 177, 275.
- [12] V. H. G. Phan, T. Thambi, M. S. Gil, D. S. Lee, *Polymer* **2017**, 109, 38.
- [13] R. Wang, Z. Yang, J. Luo, I.-M. Hsing, F. Sun, *Proc. Natl. Acad. Sci. USA* **2017**, 114, 5912.
- [14] H. Shigemitsu, T. Fujisaku, W. Tanaka, R. Kubota, S. Minami, K. Urayama, I. Hamachi, *Nat. Nanotechnol.* **2018**, 13, 165.
- [15] Z. Zhang, C. Liu, C. Yang, Y. Wu, F. Yu, Y. Chen, J. Du, *ACS Appl. Mater. Interfaces* **2018**, 10, 8546.
- [16] V. Delplace, A. Ortin-Martinez, E. L. S. Tsai, A. N. Amin, V. Wallace, M. S. Shoichet, *J. Controlled Release* **2019**, 293, 10.
- [17] H. K. Awada, D. W. Long, Z. Wang, M. P. Hwang, K. Kim, Y. Wang, *Biomaterials* **2017**, 125, 65.
- [18] J. Dai, W. Long, Z. Liang, L. Wen, F. Yang, G. Chen, *Drug Dev. Ind. Pharm.* **2018**, 44, 89.
- [19] M. H. Hettiaratchi, T. Rouse, C. Chou, L. Krishnan, H. Y. Stevens, M.-T. A. Li, T. C. McDevitt, R. E. Guldberg, *Acta Biomater.* **2017**, 59, 21.
- [20] K. F. Bruggeman, Y. Wang, F. L. Maclean, C. L. Parish, R. J. Williams, D. R. Nisbet, *Nanoscale* **2017**, 9, 13661.
- [21] G. Lokhande, J. K. Carrow, T. Thakur, J. R. Xavier, M. Parani, K. J. Bayless, A. K. Gaharwar, *Acta Biomater.* **2018**, 70, 35.
- [22] L. H. Nguyen, M. Gao, J. Lin, W. Wu, J. Wang, S. Y. Chew, *Sci. Rep.* **2017**, 7, 42212.
- [23] A. N. Steele, L. Cai, V. N. Truong, B. B. Edwards, A. B. Goldstone, A. Eskandari, A. C. Mitchell, L. M. Marquardt, A. A. Foster, J. R. Cochran, S. C. Heilshorn, Y. J. Woo, *Biotechnol. Bioeng.* **2017**, 114, 2379.
- [24] T. Jiang, S. Shen, T. Wang, M. Li, B. He, R. Mo, *Nano Lett.* **2017**, 17, 7447.
- [25] E. Anitua, A. Pino, M. Troya, P. Jaén, G. Orive, *J. Mater. Sci.: Mater. Med.* **2017**, 29, 7.
- [26] R. Waters, P. Alam, S. Pacelli, A. R. Chakravarti, R. P. H. Ahmed, A. Paul, *Acta Biomater.* **2018**, 69, 95.
- [27] D. Mertz, S. Harlepp, J. Goetz, D. Bégin, G. Schlatter, S. Bégin-Colin, A. Hébraud, *Adv. Ther.* **2020**, 3, 1900143.
- [28] F. Pertont, M. Tasso, G. A. Muñoz Medina, M. Ménard, C. Blanco-Andujar, E. Portiansky, M. B. F. van Raap, D. Bégin, F. Meyer, S. Bégin-Colin, D. Mertz, *Appl. Mater. Today* **2019**, 16, 301.
- [29] J. Bizeau, A. Adam, C. Nadal, G. Francius, D. Siniscalco, M. Pauly, S. Bégin-Colin, D. Mertz, *Int. J. Pharm.: X* **2022**, 4, 100130.
- [30] B. Li, M. Criado-Gonzalez, A. Adam, J. Bizeau, C. Mélar, A. Carvalho, S. Bégin, D. Bégin, L. Jierry, D. Mertz, *ACS Appl. Nano Mater.* **2022**, 5, 120.
- [31] S. Sugio, A. Kashima, S. Mochizuki, M. Noda, K. Kobayashi, *Protein Eng., Des. Sel.* **1999**, 12, 439.
- [32] G. I. Berglund, G. H. Carlsson, A. T. Smith, H. Szöke, A. Henriksen, J. Hajdu, *Nature* **2002**, 417, 463.
- [33] E. E. Kim, H. W. Wyckoff, *J. Mol. Biol.* **1991**, 218, 449.
- [34] M. Muraki, S. Goda, H. Nagahora, K. Harata, *Protein Sci.* **1997**, 6, 473.
- [35] J. Bizeau, A. Adam, S. Bégin, D. Mertz, *Eur. J. Inorg. Chem.* **2021**, 2021, 4799.
- [36] F. Pertont, S. Harlepp, G. Follain, K. Parkhomenko, J. G. Goetz, S. Bégin-Colin, D. Mertz, *J. Colloid Interface Sci.* **2019**, 542, 469.
- [37] P. Duenas-Ramirez, C. Bertagnolli, R. Müller, K. Sartori, A. Boos, M. Elhabiri, S. Bégin-Colin, D. Mertz, *J. Colloid Interface Sci.* **2020**, 579, 140.
- [38] A. Adam, K. Parkhomenko, P. Duenas-Ramirez, C. Nadal, G. Cotin, P.-E. Zorn, P. Choquet, S. Bégin-Colin, D. Mertz, *Molecules* **2021**, 26, 971.
- [39] A. Adam, S. Harlepp, F. Ghilini, G. Cotin, B. Freis, J. Goetz, S. Bégin, M. Tasso, D. Mertz, *Colloids Surf., A* **2022**, 640, 128407.
- [40] G. Schulz-Ekloff, J. Rathouský, A. Zukal, *Int. J. Inorg. Mater.* **1999**, 1, 97.
- [41] Y. Wang, F. Caruso, *Chem. Mater.* **2005**, 17, 953.
- [42] A. Micsonai, F. Wien, É. Bulyáki, J. Kun, É. Moussong, Y.-H. Lee, Y. Goto, M. Réfrégiers, J. Kardos, *Nucleic Acids Res.* **2018**, 46, W315.
- [43] A. Micsonai, F. Wien, L. Kernya, Y.-H. Lee, Y. Goto, M. Réfrégiers, J. Kardos, *Proc. Natl. Acad. Sci. USA* **2015**, 112, E3095.
- [44] A. Micsonai, É. Bulyáki, J. Kardos, in *Structural Genomics* (Eds: Y. W. Chen, C.-P. B. Yiu), Springer US, New York, NY **2021**, pp. 175–189.
- [45] P. K. Smith, R. I. Krohn, G. T. Hermanson, A. K. Mallia, F. H. Gartner, M. D. Provenzano, E. K. Fujimoto, N. M. Goeke, B. J. Olson, D. C. Klenk, *Anal. Biochem.* **1985**, 150, 76.
- [46] J. M. Walker, in *The Protein Protocols Handbook* (Ed. J. M. Walker), Humana Press, Totowa, NJ **2009**, pp. 11–15.
- [47] B. Meloun, L. Morávek, V. Kostka, *FEBS Lett.* **1975**, 58, 134.
- [48] R. M. Lawn, J. Adelman, S. C. Bock, A. E. Franke, C. M. Houck, R. Najarian, P. H. Seeburg, K. L. Wion, *Nucleic Acids Res.* **1981**, 9, 6103.
- [49] A. Dugaiczky, S. W. Law, O. E. Dennison, *Proc. Natl. Acad. Sci. USA* **1982**, 79, 71.
- [50] K. G. Welinder, *FEBS Lett.* **1976**, 72, 19.
- [51] N. C. Veitch, *Phytochemistry* **2004**, 65, 249.
- [52] M. Besman, J. E. Coleman, *J. Biol. Chem.* **1985**, 260, 11190.
- [53] J. C. Hua, J. Berger, Y. C. Pan, J. D. Hulmes, S. Udenfriend, *Proc. Natl. Acad. Sci. USA* **1986**, 83, 2368.
- [54] H. Weissig, A. Schildge, M. F. Hoylaerts, M. Iqbal, J. L. Millán, *Biochem. J.* **1993**, 290, 503.
- [55] M. J. Castañón, W. Spevak, G. R. Adolf, E. Chlebowicz-Śledziewska, A. Śledziewski, *Gene* **1988**, 66, 223.
- [56] L. P. Chung, S. Keshav, S. Gordon, *Proc. Natl. Acad. Sci. USA* **1988**, 85, 6227.
- [57] K. Yoshimura, A. Toibana, K. Nakahama, *Biochem. Biophys. Res. Commun.* **1988**, 150, 794.